8-2022

Speed of Small Droplets on Repellent Surfaces

Addison J. Litton
Utah State University

SPEED OF SMALL DROPLETS ON REPELLENT SURFACES

by

Addison J. Litton

A thesis submitted in partial fulfillment
of the requirements for the degree

of

MASTER OF SCIENCE

in

Mechanical Engineering

Approved:

Tadd T. Truscott, Ph.D. Major Professor	Jesse Belden, Ph.D. Committee Member
Som Dutta, Ph.D. Committee Member	Greg Droge, Ph.D. Committee Member

D. Richard Cutler, Ph.D.
Vice Provost of Graduate Studies

UTAH STATE UNIVERSITY
Logan, Utah

2022

ABSTRACT

Speed of Small Droplets on Repellent Surfaces

by

Addison J. Litton, Master of Science

Utah State University, 2022

Major Professor: Tadd T. Truscott, Ph.D.
Department: Mechanical and Aerospace Engineering

Water droplets will slide or roll down an inclined plate if the surface conditions of the plate inhibit surface adhesion. Two such conditions are when the plate is coated with a superhydrophobic coating or if the plate is heated to the Liedenfrost point. The superhydrophobic surface supports the droplet on the top of tiny ridges on the surface and results in the droplet rolling down the incline. The Leidenfrost surface supports the droplet by evaporating a small amount of the fluid that forms a vapor layer between the droplet and the plate, allowing the droplet to slide on the vapor layer down the incline (note: rolling may still occur). The speed of the droplet is likely a function of the velocity, diameter, and density. However, if the droplet is sliding rather than rolling the speed of the droplet should change and potentially be unaffected by viscosity differences. Herein, we compare multiple fluid types on both surface types at different inclined angles. Droplets are consistently released on an inclined plate and tracked with high speed video. Comparisons are made using velocity and acceleration inferred from position data. The data reveal that water droplets have velocities faster than more viscous droplets while Leidenfrost surfaces tend to inhibit the effect of viscosity. There are cases in both surface types where the droplets can travel faster than the potential energy estimate, which indicates that some droplets may

experience thrust. Droplets on Leidenfrost surfaces experience this between 2° and 4° while the same occurs on superhydrophobic surfaces for water only above 6°.

(56 pages)

PUBLIC ABSTRACT

Speed of Small Droplets on Repellent Surfaces

Addison J. Litton

A droplet of fluid can slide or roll down an angled surface if the droplet doesn't stick to the plate (e.g., droplets on glass). The most common surface to allow for such this motion are hydrophobic surfaces. One example is a freshly waxed car where the rain beads up and rolls off. Another example is if a pan is heated to a high enough temperature then when small amounts of water are added the droplet will skitter around on the surface for a moment before boiling away. This high temperature effect where droplets rest on a vapor layer underneath cause by the heat is called the Leidenfrost point. One might ask which surface type will encourage a droplet to go down the surface fastest? Herein an analysis and comparison of droplets on both of these types of surfaces is performed, with consideration given to the size of the droplet, the angle of the surface, and the type of droplet by varying the relative thickness or viscosity. The droplet velocity and acceleration are compared and the hydrophobic surfaces with water have the most consistent high velocities. However, making the droplets more viscous slows down the droplets on hydrophobic surface more effectively than on Leidenfrost ones. Finally, both surfaces can produce a form of thrust if conditions are right.

CONTENTS

LIST OF TABLES

LIST OF FIGURES

CHAPTER 1

INTRODUCTION

All surfaces have some roughness to them. Even the most polished surface have high and low spots to some degree. These little surface deformations are the cause of friction between objects. When one of those objects is a fluid, some of the fluid can fall into those small gaps between local high spots. If that surface is sloped as the droplet tends down that slope it will begin to roll as it pulls itself from those cavities. Mahadevan and Pomeau [2] identified rolling as one of the 2 types of motion that a fluid droplet can have. The other type of motion is sliding. While rolling involves the viscous forces acting against the movement of the droplet as it spirals down the surface, a sliding drop moves without internal motion. This sliding action can been seen when water is poured onto a very hot skillet [3]. As a portion of the water begins to boil, the newly formed water vapor forms a boundary between the remaining fluid and the skillet. This is called the Leiden-frost effect. When the droplet is resting on its vapor there is expected to be very little internal motion, less rolling more sliding, and so the speed of the droplet is expected to be much higher. Some of the research cited above has shown this. Some further research is to be done to show if a droplet on a sufficiently hydrophobic surface can achieve the same sliding and higher velocities without need for the incredibly high temperatures.

A question then arises due to the odd nature of mercury. On many surfaces, mercury will ball to form small spheres and minimize its contact with the surface. This can be measured as the contact angle of the fluid with the surface. In a Leidenfrost case, that contact angle will be 180°. New work has been done in hydrophobic coatings for surfaces which also increase the contact of fluids like water to near 180°. Thus the question becomes, can a hydrophobically coated surface allow for droplets to slide minimizing friction [4] to almost zero as in Leidenfrost conditions [3].

Work done by Boiullant et. al [5] showed that small droplets on a Leidenfrost surface can self propel. This could be cause for acceleration of the droplets down the plate. However, this was shown to only effect droplets below the capillary length ($r < 1.4$ mm). Here, we focus on droplets between 1.75 and 2.16 mm.

Another consideration to make when puzzling this question, is what affect the viscosity of the fluid will have on the droplet. Higher viscosity fluids will resist internal rotation more which may have a slowing effect by lowering the rotation. The lowered rotation may lead to more sliding since the droplet will be less prone to sink into the cavities in the surface. If the first is true that more viscous fluids are slower, then will non-Newtonian shear thinning fluids overcome the effect. The purpose of this work is to answer these questions.

CHAPTER 2

OBJECTIVES

This thesis will investigate the velocity of droplets traveling down a small angled inclined plate. Six fluids of different viscosity are evaluated on two surface treatments at four angles.

The hypothesis is that the terminal velocity and acceleration of a droplet on an inclined plated (small angle, $< 8^{\circ}$) heated to the liedenfrost point is less dependent on viscosity than a similar droplet on a superhydrophic surface. In other words, a less viscous fluid should be faster on a hydrophobic surface and viscosity shouldn't affect velocity as much on a leidenfrost surface. Further, there should be a difference between constant shear and shear thinning fluids under both circumstances.

Based on this hypothesis, the main objectives of this thesis are as follows:

1. Design and build a novel release mechanism that allows for consistent droplet release with minimal initial vibration of the droplets.

2. Collect high-speed video to determine the acceleration and terminal velocity of the droplet as it travels down the plate.

3. Determine the effect of viscosity on the velocity down an inclined plate for both Newtonian and non-Newtonian fluids.

4. For each fluid measure the velocity and acceleration as it relates to the following effects:

    Angle

    Leidenfrost vs. Superhydrophobic surfaces

    Viscosity

    Diameter

CHAPTER 3

APPROACH

Two separate fluids will be tested, distilled water mixed with xanthan gum, which creates a non-Newtonian shear thinning fluid, and distilled water mixed with glycerol, which creates a Newtonian Fluid. Distilled water will also be run as a baseline. To compare the fluids to one another, 144 tests were devised across four factors to determine the effects of each parameter on the droplets. All tests were repeated and recorded at least twice to give a total of 288 data points. See table 3.1 for the break down of these tests.

Table 3.1: Test parameters and their test values. LiedenFrost point values are estimated from literature [1]. Viscosity values for Xanthan Gum can be found in figure 3.2

Fluid Types (LiedenFrost Point)	Viscosity (mm^2/s)	Surface Tension (N/m)	(μ L)	Plate Types	Plate Angle (θ°)
Distilled Water (193°C)	1	0.076	22.5	Heated 300°C	2
85%wt Glycerol (240°C)	110.0 [6]	0.076	32.5	Hydrophobic 120°	4
60%wt Glycerol (208°C)	10.8 [6]	0.076	42.5		6
0.5%wt Xanthan (195°C)	200	0.076			8
0.3%wt Xanthan (195°C)	100	0.076			
0.1%wt Xanthan (195°C)	10	0.076			

3.1 Droplets

The fluids are prepared by slowly adding the desired amount of glycerol or xanthan gum to a beaker of distilled water. This beaker is gently warmed on a hot plate and constantly stirred to achieve a uniform solution. The % weight concentrations were selected in order to have similar viscosity between the fluids, the 0.1% xanthan gum correlates to 60% glycerol and 0.3% xanthan gum correlates to 85% glycerol. The 0.1% xanthan gum would have correlated roughly to a 100% glycerol solution, but this solution proved difficult to test because it remained stuck to the plate and would not roll (superhydrophobic plate). This

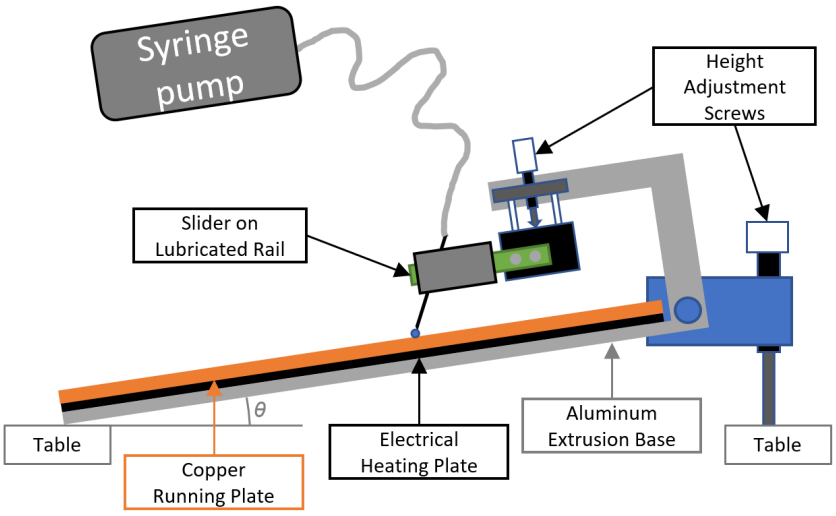

Fig. 3.1: Simplified drawing of experimental setup.

did not hinder the 0.5% xanthan gum from being tested, likely due to its shear thinning behavior.

Fluids were stored in a refrigerator and allowed to come to room temperature before testing began. The fluid was then pulled into a clear tube and syringe which was loaded into a syringe pump. The clear color was chosen to allow for the inspection of the fluid to ensure no air droplets were trapped which may have affected the droplet size. The pump was calibrated based on the ID of the syringe being used so as to be able to extrude a droplet of a known volume. This volume can be confirmed using the camera data later on by measuring the diameter of the droplet. With droplets extruded onto the plate, the needle was removed allowing the droplet to travel freely down the surface of the plate.

3.2 Droplet Release Mechanism

A calibrated syringe pump connected via surgical tubing to a small diameter needle. The needle is securely fastened to a clip on a lubricated rail. This allowed for the needle to be positioned according to the camera setup, such that the needle would be on the far edge of the first camera field of view. The assembly was connected to an adjustable stage. This stage could be raised and lowered using a micrometer dial allowing for slow and steady

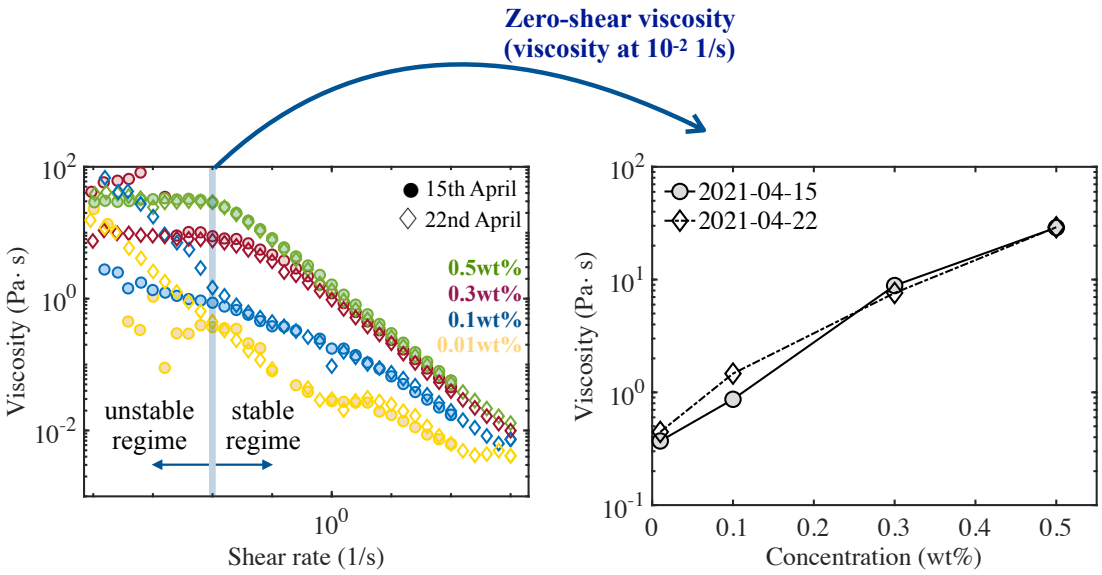

Fig. 3.2: Plot of Viscosity vs shear rate of xanthan gum solutions. Measurements were taken on the same solution on different days to show that the fluid was stable for testing over a week.

movement of the needle. The needle was positioned close to the surface of the plate such that the droplet could be held in place between the needle and plate. If the gap between the needle tip and the plate was too great, the droplet would come off the needle before it was desired.

Once the droplet was made and the cameras ready to trigger, the needle was gently moved away from the plate. Gravity would then pull the droplet from the needle. After release the droplet oscillates anywhere from 650 ms for water to only 15 ms for 85% glycerol and 0.5% xanthan. The droplet then freely glided down the plate. The droplet position was recorded by the camera. The initial motion was recorded to view the oscillation of the droplet, while the motion at the end of the plate was used to determine the droplet velocity.

3.3 Experimental Surfaces

Two one meter copper running plates where prepared for the experiment by carefully polishing each to a mirror finish. This polishing was done by sanding the surface of the plate with increasingly finer grit (i.e., 400 initial only, then 800, 1200, 2000, 3000) using an orbital sander and an aluminum cutting fluid. Between test days a repolishing was accomplished by starting at 800 grit up to 3000 in particular when the plate was cooled and oxidation was present. In the case of hydrophobic coatings, only if the surface was damaged would the plate be repolished. Instead, if the surface was damaged then the coating was removed and a new coating applied. The one meter length was selected based on work by [4] that determined terminal velocity of a droplet on a small angle plate should happen in less than one meter. A plate was left as just a polished surface for the Leidenfrost experiment, while the other was coated in WX-2100 hydrophobic spray (120°). The coating was allowed to dry in a fume hood before testing.

Depending on the current test, either the polished plate or the coated one, was placed on top of a heater plate which in both cases acted as a flat reference for the experiment. For the cases of Leidenfrost tests, the plate was then heated to 300 C, which was monitored and controlled by a micro-controller. The test plate and heater plate were also placed on top of a piece of aluminum extrusion for mounting purposes. These three plates can be

seen in Figure 3.1. The aluminum extrusion is then connected by a single bolt to a screw similar to the one used in the droplet release mechanism, but larger. This single connection point allowed the plate to rotate around to provide a sloped angle. By using this point and resting the other end on the table, the angles desired for the experiment were easily achieved. The attachment bolt could be tightened to adjust the angle of the plate front to back. This could level the plate such that the droplet path was more parallel to the camera images, minimizing out of plane motion.

The plate developed a significant amount of thermal scaling after cooling from the Leidenfrost test cases. This was rectified by following the same polishing process as the initial setup so that each subsequent test would be equal to the first. In the hydrophobic case, extreme care is taken to not scratch or even touch the surface to avoid damaging it. Damage can easily be seen by droplets stopping or slowing on the surface. The plate was examined and retreated often. If damage was severe enough, the plate was cleaned fully following the same setup procedure and re-coated. All this was done to ensure a consistent testing surface across multiple tests and days.

3.4 Image capture and processing

The droplet is recorded using Three Photron SA3 cameras mounted on a tripod each adjusted so as to look across the top of the plate minimizing the width of the plate in the image. The cameras were placed one at the front to observe the release and subsequent oscillation of the early droplet, the second in the middle of the plate overlapping the first's view, and the third at the end of the plate. During some runs of the droplet, the second camera was mounted above the plate to track the path of the droplet from just after release to verify it was true, or close to parallel to the camera view. Each camera is equipped with a 50 mm macro lens. The lens apertures are set to best illuminate the droplet from the background. The videos are recorded with the Photron Fastcam Viewer 3 software. The cameras are set at 2000 fps. The resolution of the cameras varies depending on the angle of the plate and where along the path of the droplet they are placed. The cameras are set to have a shutter speed of 1/7500 sec. The droplets are back lit by an LED light bank.

The images are processed using MATLAB. A data set begins, with the droplet just out of frame. This first image is taken and saved as the baseline. The baseline image is called up and the experimenter selects 2 points along the top surface of the plate. This is done in comparison with the stated angle of the plate to ensure that angle is accurate to the measured angle. This angle is saved for later.

The first 30-80 frames are thrown out depending on droplet size and plate angle. This is done so that the whole droplet is in the field of view. This is considered time step 0 ($t0$). All images have the baseline subtracted from them. Since the cameras are very steady over this short time, this leaves only the droplet on a field of black, making it easier to find the centroid and top of the droplet.

The image is rotated by the predetermined value such that the path of the droplet is mostly one dimensional. The image is then cropped to reduce data being manipulated. The image is binarized by setting all positive pixels to 1, since the background is already 0. The centroid of the drop is determined and saved. For analysis done on the release of the droplet a bounding box is also found and the height and width of that box is saved. This process is repeated automatically for all images in the data set ranging from 200 images on the highest slope, to 1100 images on the lowest. See Figure 3.3 for a sample set of this process.

Time steps are determined by the settings of the camera. A calibration image taken at the beginning of the experiment is used to determine the number of pixels per millimeter. This is accomplished by stretching a tape measure across the top of the plate and taking a picture. This image is then rotated based on the baseline image and the user selects two of the tick marks on the tape measure and enters the length. The value of pixels per millimeter is then saved and used to convert the position values found earlier to centimeters along the plate.

The time step data along with the position of the centroid at each point is then entered into a spline code provided by Brenden Epps [7]. The code fits a spline to the data which can then be interpreted to find velocity and acceleration at each point. Near the end of

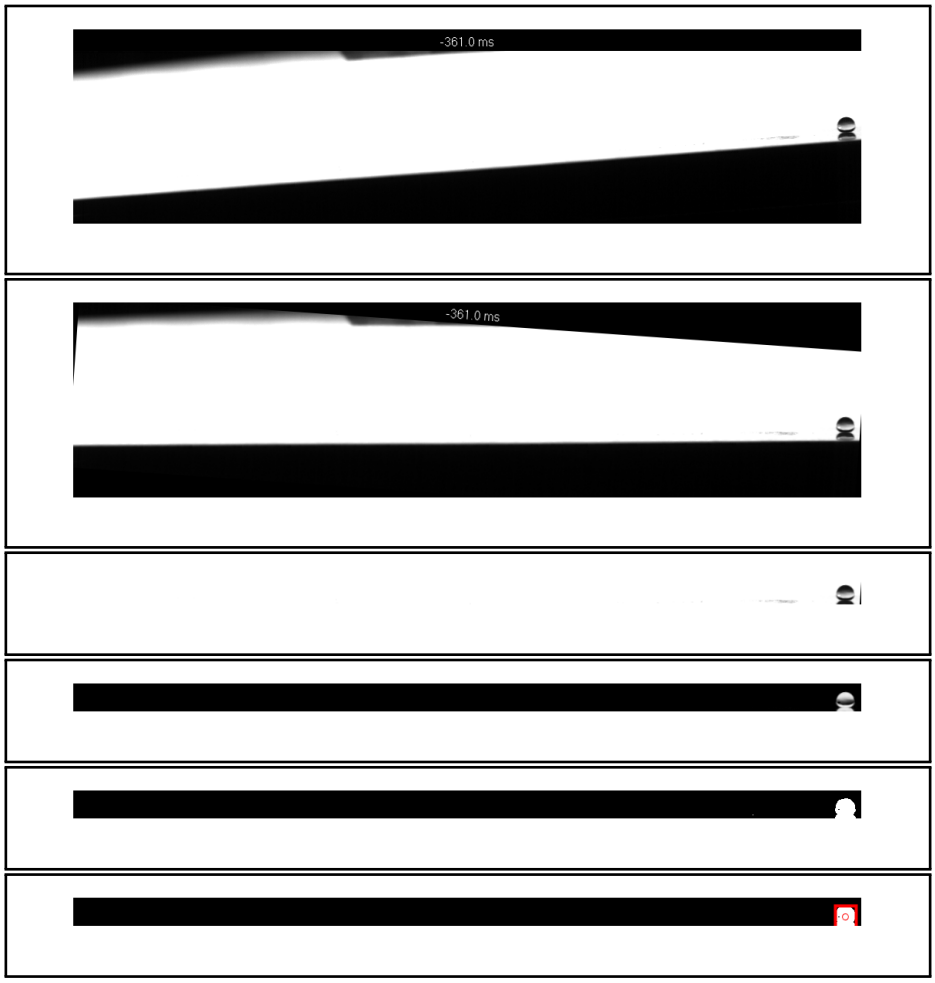

Fig. 3.3: Image processing steps changed for display purposes: Base image, rotated, cropped, background subtracted, binarized, centroid and bounding box found.

the plate where the droplet is assumed to be at terminal velocity, the mean and standard deviation of the droplet velocities and accelerations are determined.

A subset of the data will have the images near the release of the droplet observed. This is done to observe initial oscillation of the droplet. this is done by finding a bounding box whose height and width are taken and used as an aspect ratio. Aspect ratio is determined as the width of the bounding box or droplet over the height of the droplet in any given frame. The initial oscillation of the droplet is tracked to determine how quickly that vibration dampens out.

After the testing is complete the droplet data will be analyzed looking for trends in the data.

CHAPTER 4

RESULTS

The first issue to examine is the reliability of the data. Figure 4.1 reveals the final velocity versus angle of the plate for a 22.5 µL droplet of all the droplet types. The colors represent the droplet type, X marks phobic cases and O marks Leiden-frost ones. The left and right plots show two separate runs of each test. The data are extremely similar, showing the reliability of the testing. Two other droplet diameters were also compared this way 32.5 µL in figure 4.2 and 42.5 µL in figure 4.3. The following discussion will look at trends, and implications of the data.

4.1 Velocity

The hydrophobic test cases performed as expected in figures 4.1, 4.2, & 4.3. As the angle of the plate increased, the velocity of the droplet increases. Also, viscosity plays a large role in that final speed, where the higher viscosity droplets are slower. The non-Newtonian cases (i.e., xanthan gum) have a viscosity that decreases with shear (aka shear thinning). As they roll down the ramp their viscosity decreases allowing them to roll a bit faster than the glycerin cases. Further, the highest concentrations of both glycerin and xanthan gum had the highest viscosities and as expected rolled the slowest down the incline.

The Leiden-frost trend is not as obvious as the hydrophobic cases. In general, the Leiden-frost cases have the same final velocities for each angle despite their viscosity. This is partially expected as the vapor layer should decrease the droplet dependence on rolling and viscous resistance. At the lower angles 2° and 4° it seems that the glycerin cases have velocities that match the trend at 6° and 8°. However, the other cases (water and xanthan gum) are even faster than the 6° and 8° plates. A simple energy balance on the droplet reveals that the maximum speed of the droplets without drag or shear should be $\sqrt{2glsin(\theta)}$. Since the droplets are faster than this theoretical maximum it is necessary

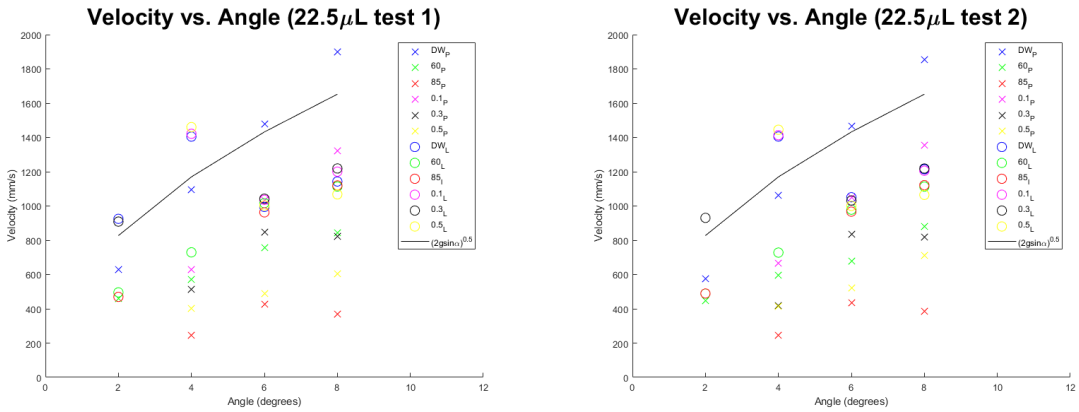

Fig. 4.1: Plots show the consistency of testing with 22.5 μ L droplets. Error is on the order of the marker size with the error in the $y = \pm 15$mm/s, and the error in the $x = \pm 0.05°$.

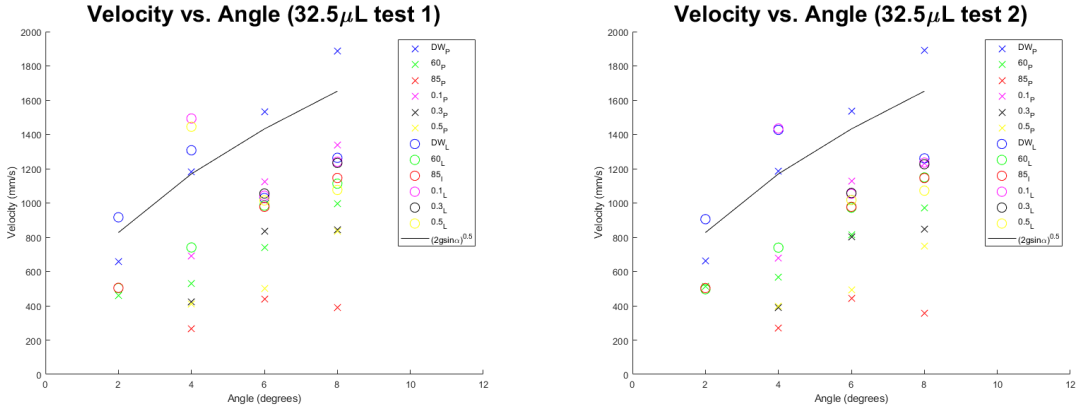

Fig. 4.2: Plots show the consistency of testing with 32.5 μ L droplets. Error is on the order of the marker size with the error in the $y = \pm 15$mm/s, and the error in the $x = \pm 0.05°$.

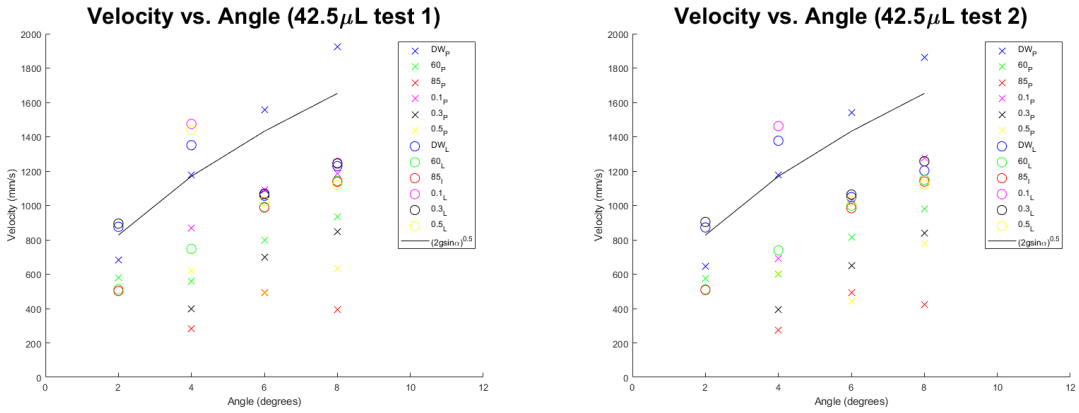

Fig. 4.3: Plots show the consistency of testing with 42.5 μ L droplets. Error is on the order of the marker size with the error in the $y = \pm 15$mm/s, and the error in the $x = \pm 0.05°$.

that another force is at play. Plotting the initial accelerations (4.7) from the release do show that the accelerations in the 4° cases are much higher than in the 6° cases. The data seems to be repeatable and at several volumes, so the reason is not yet clear. Perhaps the vapor layer has some thrust type effect on the droplet speed that is achieved somewhere between 2° and 6°. Yet, at 8° it the velocities are again nearing the same values as the 4° cases. Boiullant et. al [5] found that certain sized droplets on a Leiden-frost surface will self propel if the angle of the plate is small enough. That is to say the direction of travel of the droplet is random up until a certain threshold when the gravitational forces dominate and the droplets will then tend in the one direction. This could explain the additional speed, however, Boiullant et. al noticed this only held for small droplets (i.e., smaller than this study). Since the droplets here are on a larger incline it is possible that the shape of the droplet could lead to an altered shape that could be conducive to an increased inclination that would accelerate the droplet or angle similar to observations of [5]. This shape could perhaps only form effectively at small plate angles where the gravitational effects are large enough to deform the droplets but not so large as to dominate them. More work could be done using interferometry and PIV to determine the shape of the droplets in these cases and to identify the mechanics at work.

Finally, at 6° and 8° in the superhydrophobic cases of water only, the droplets also have velocities faster than the potential energy predicts. Again it is possible that here the incline is large enough to cause some sort of increased angle deformation similar to [5] or something else. Certainly worth further exploration.

Figures 4.4 through 4.6 show that the droplets on the hydrophobic plate behaved as expected where the higher angle paths were faster, and the higher viscosity fluids were slower. In the 2° and 4° cases this seems to be true as well for the Leiden-frost cases. The interesting point occurs after 4°, where the speed of the Leiden-frost droplet all start to bunch together, and some are even slower that the same droplet on the hydrophobic cases, namely water.

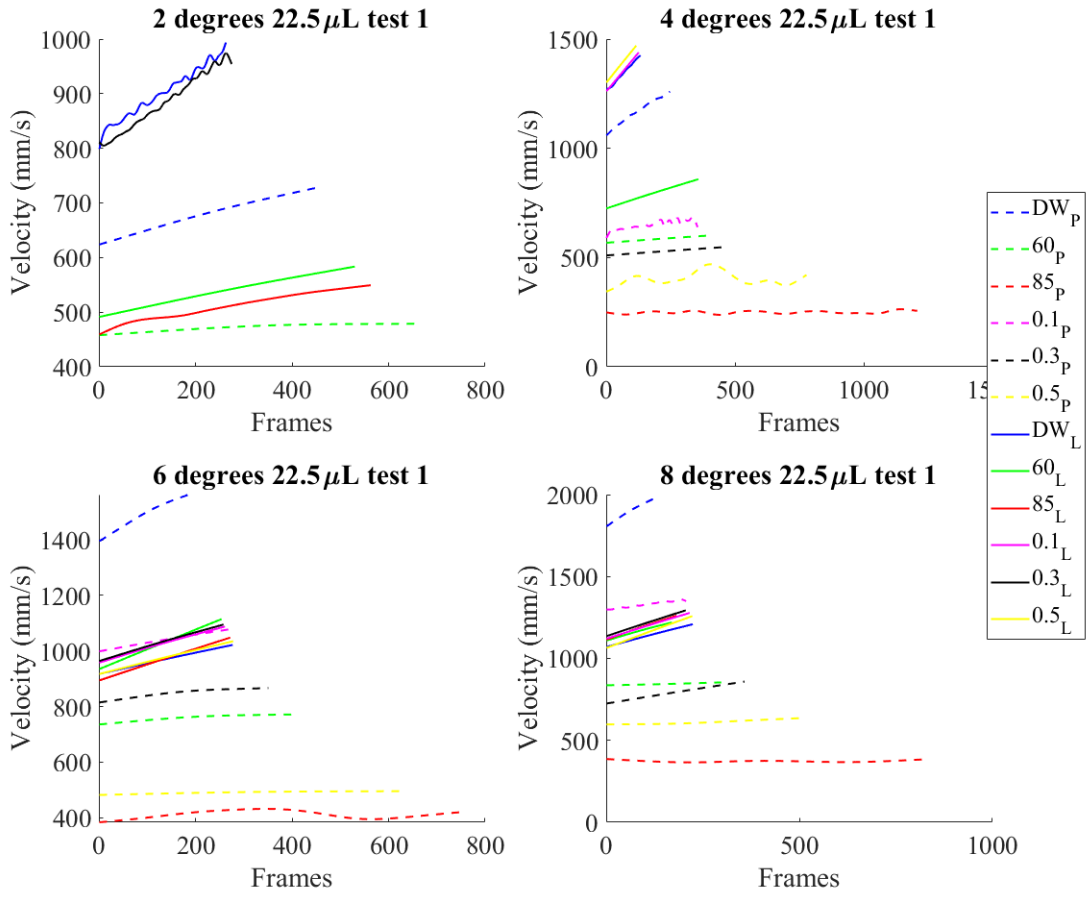

Fig. 4.4: Plot of velocities for 22.5 μL of all successful droplet types.

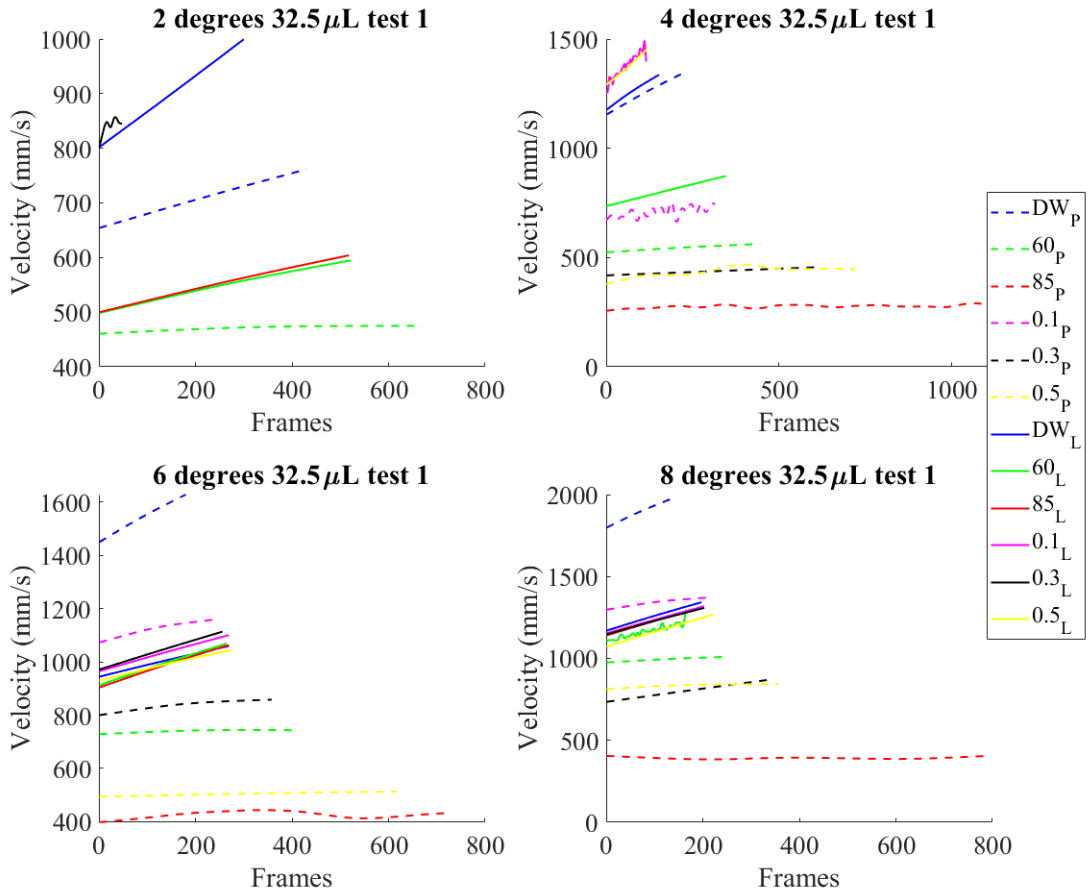

Fig. 4.5: Plot of velocities for 32.5 μL of all successful droplet types.

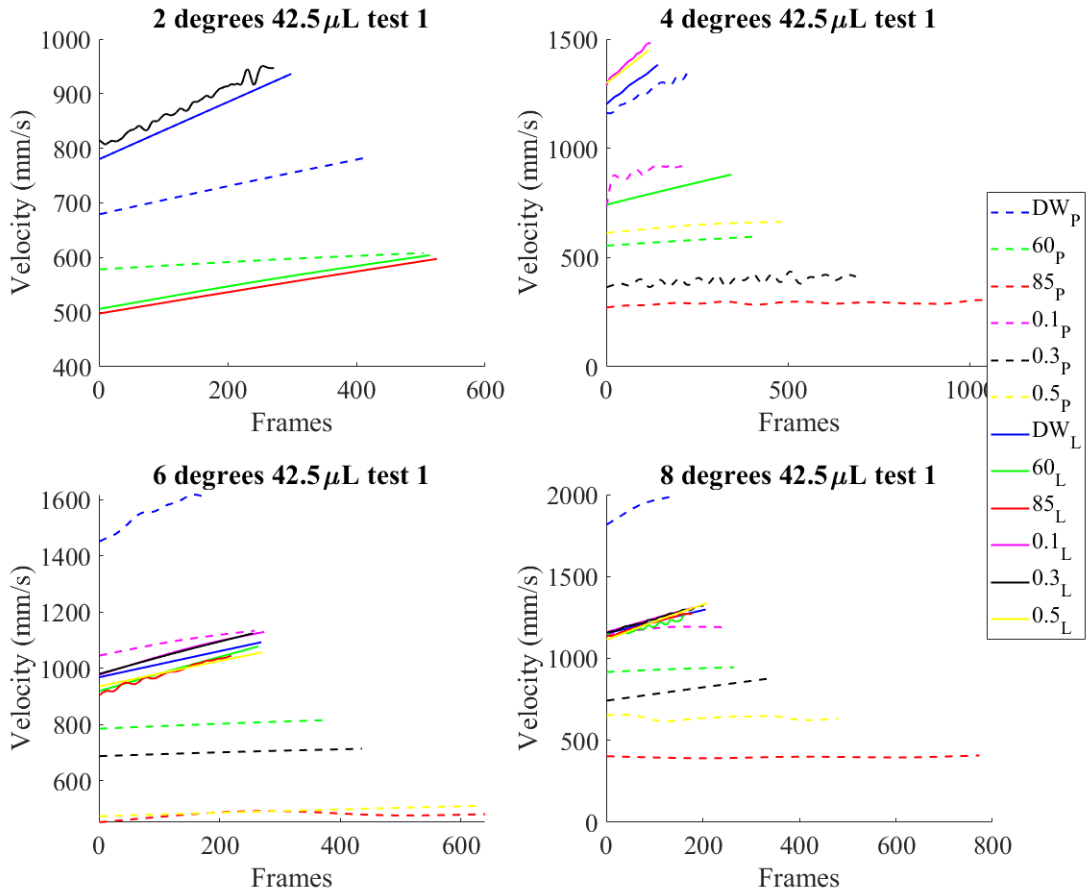

Fig. 4.6: Plot of velocities for 42.5 μL of all successful droplet types.

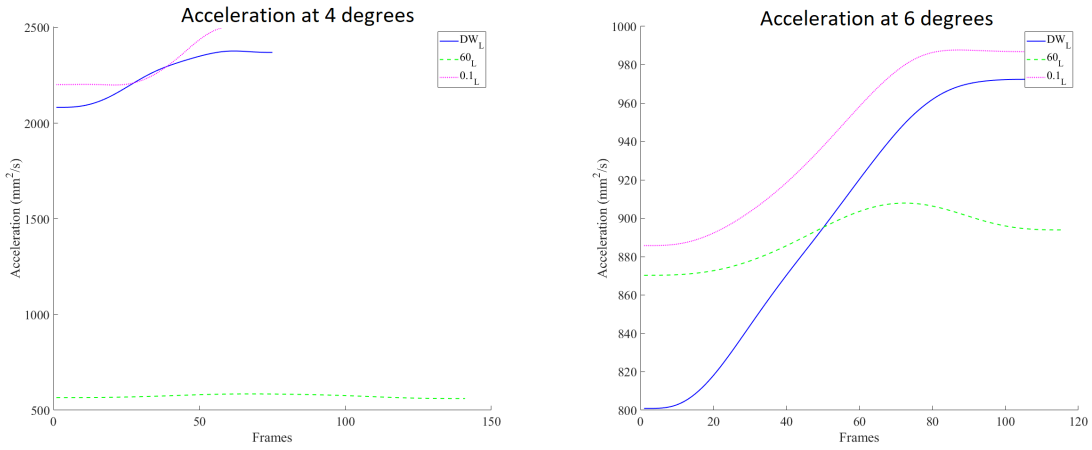

Fig. 4.7: Each of these accelerations is for 42.5 μL droplets. The higher accelerations explain the higher velocities seen at the end of the plate.

Figures 4.8, 4.9, and 4.10 zoom in on the Leiden-frost cases alone. It can be seen that there is something occurring between 4 and 6 degrees that effects the droplets speed to cause the distilled water to go from the quickest to joining the slowest of the fluids in some of the cases.

One issue with definitively proving the hypothesis of this paper is that it is based on the droplet being at terminal velocity. As the velocities of all droplets tend upward, they are perhaps not yet at terminal velocity. However, some conclusions can be drawn. At small angles droplets on a hydrophobic surface behave as expected with regards to the dependence of velocity on viscosity. The Leiden-frost surfaces provided a final velocity that was more independent of viscosity than the hydrophobic cases, although it seems there may be some ideal angles and some effect of viscosity to consider. The droplet release mechanism worked to produce consistent results. The data processing works well, even though some tweaks to the code as well as the image capture setup may improve the data.

4.2 Aspect Ratio

The aspect ratio, defined as width over height, can tell us about the droplets initial release condition as well as help confirm the size of the droplet. The aspect ratio of all the droplets should be greater than one since they are above the capillary length and thus the

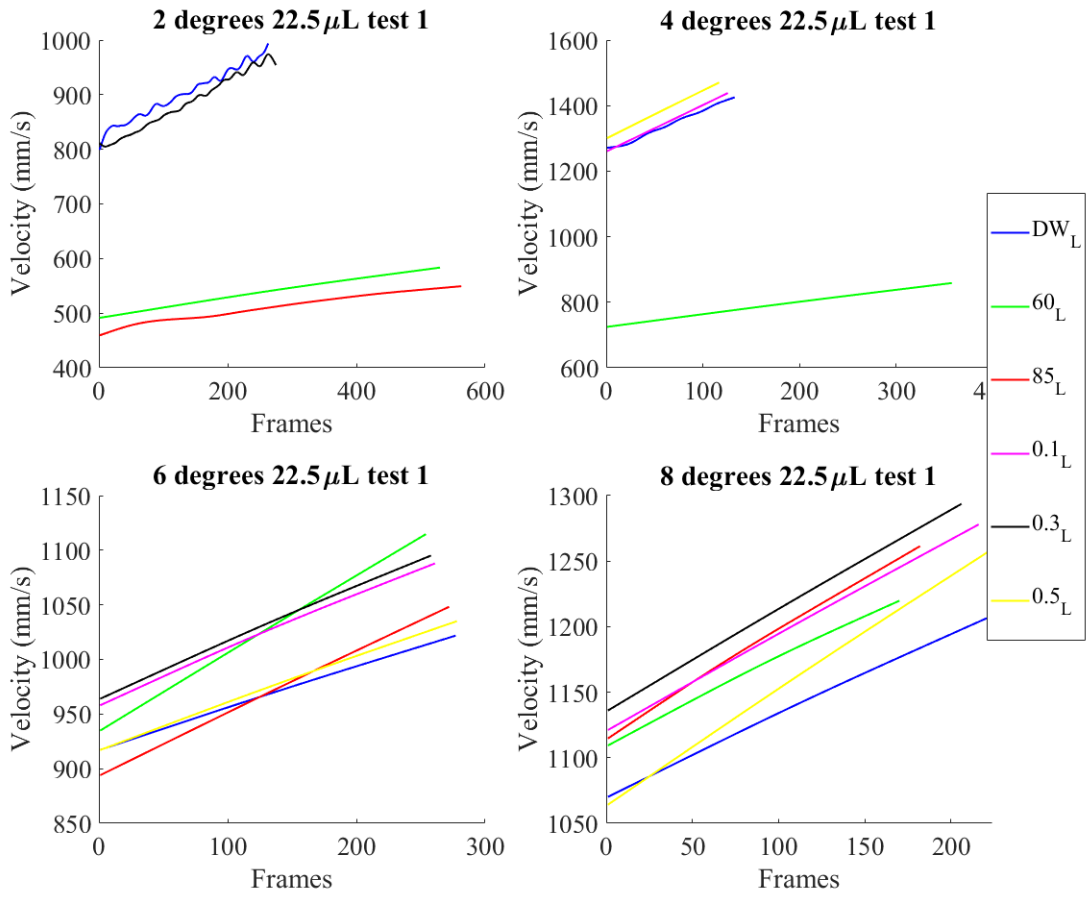

Fig. 4.8: Plot of velocities on the Leiden-frost surface for 22.5 μL of all successful droplet types.

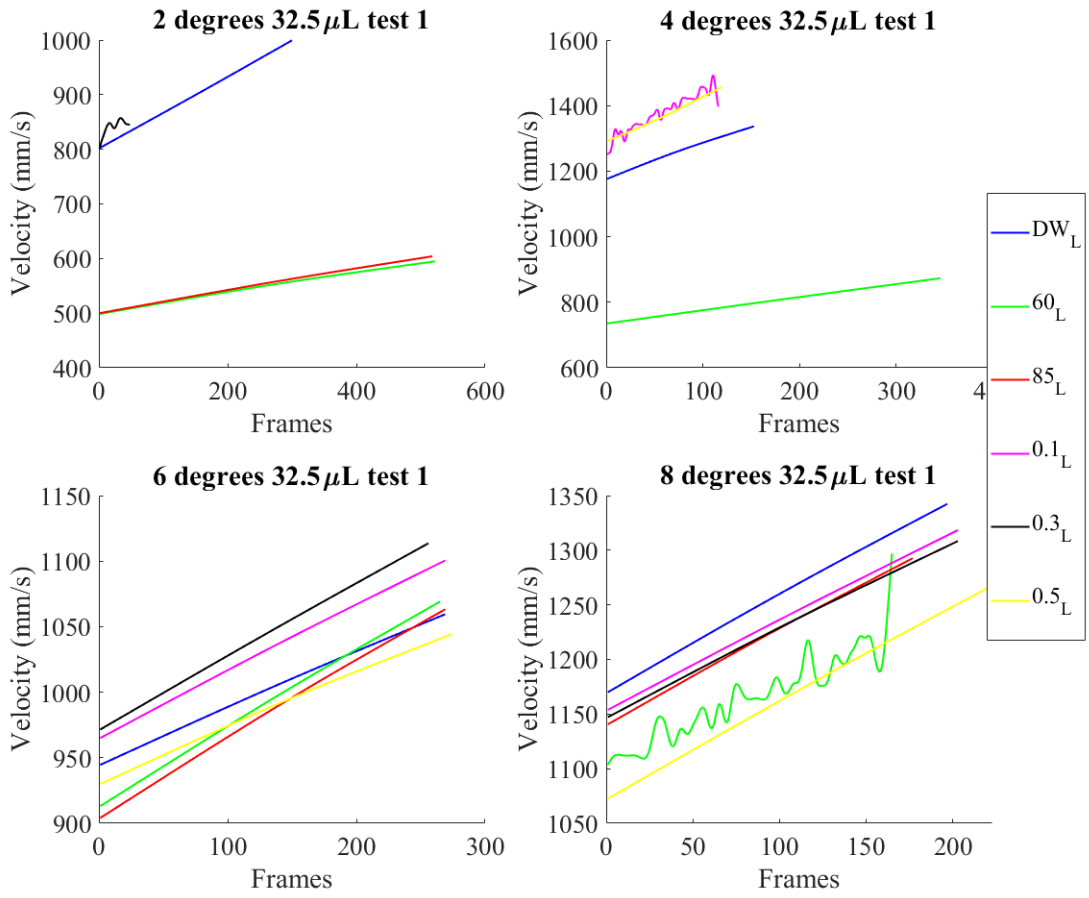

Fig. 4.9: Plot of velocities on the Leiden-frost surface for 32.5 μL of all successful droplet types.

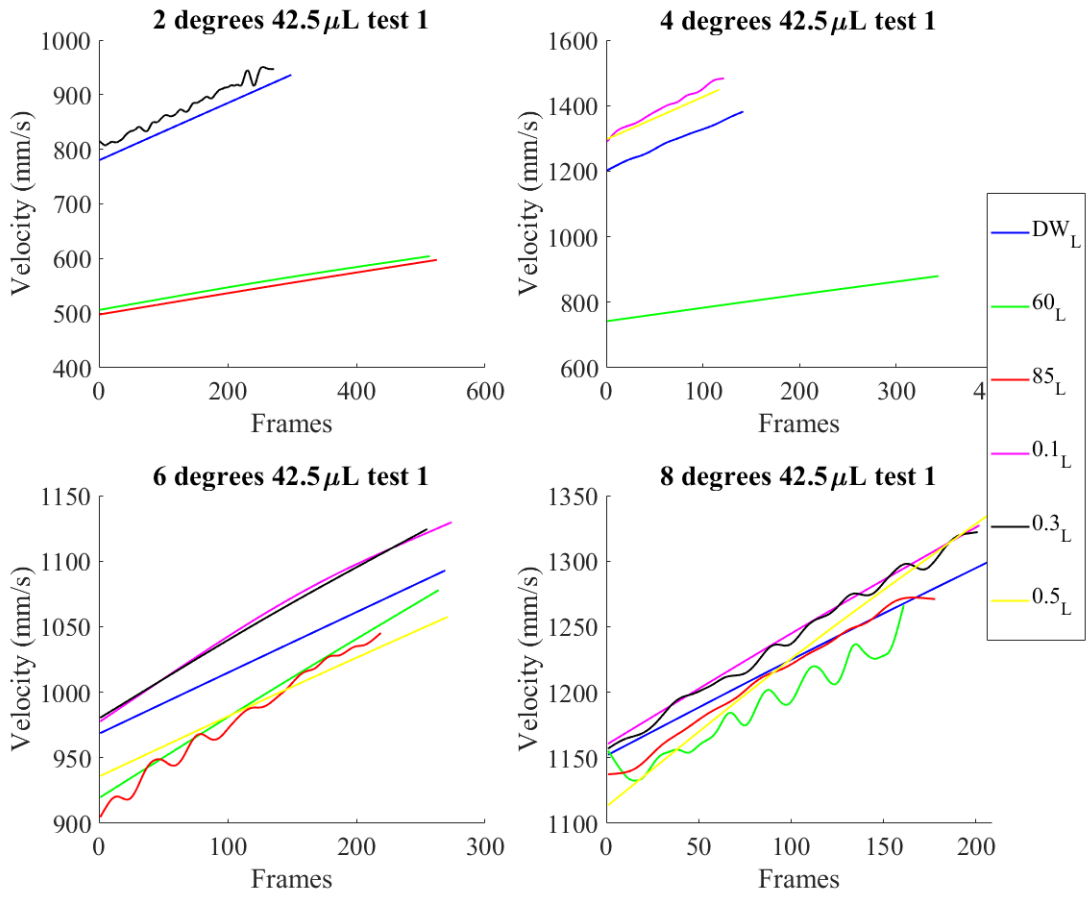

Fig. 4.10: Plot of velocities on the Leiden-frost surface for 42.5 μL of all successful droplet types.

gravitational effect outweighs the capillary effect and the droplet flattens out slightly on the plate surface.

Droplets have an initial oscillation in them due to the way they are released onto the plate as discussed in section 3.2. Figures 4.11 and 4.12 show the oscillation in the 8° plate for a 42.5 μL droplets on both the Leiden-frost and hydrophobic surfaces. More oscillation data for the other angles is in the appendix A. While some oscillation in the droplet is to be expected as the droplet bounces slightly after release, the large changes in aspect ratio as seen especially in the Leiden-frost droplet cases are larger than expected. These large changes and erratic behaviors are primarily caused by the image processing where reflections in the surface are included in the measurement. The majority of these changes occurred in the y direction, where the height of the droplet would suddenly change especially as the reflection increases with the oscillation in the y direction. This was also true of the droplets further down the plate. These same artifacts were present when droplets position and speed were determined near the end of the plate. Since these were almost all in the y direction, the x portion of the centroid is unaffected, and thus reliable enough to determine velocity and acceleration of the droplets.

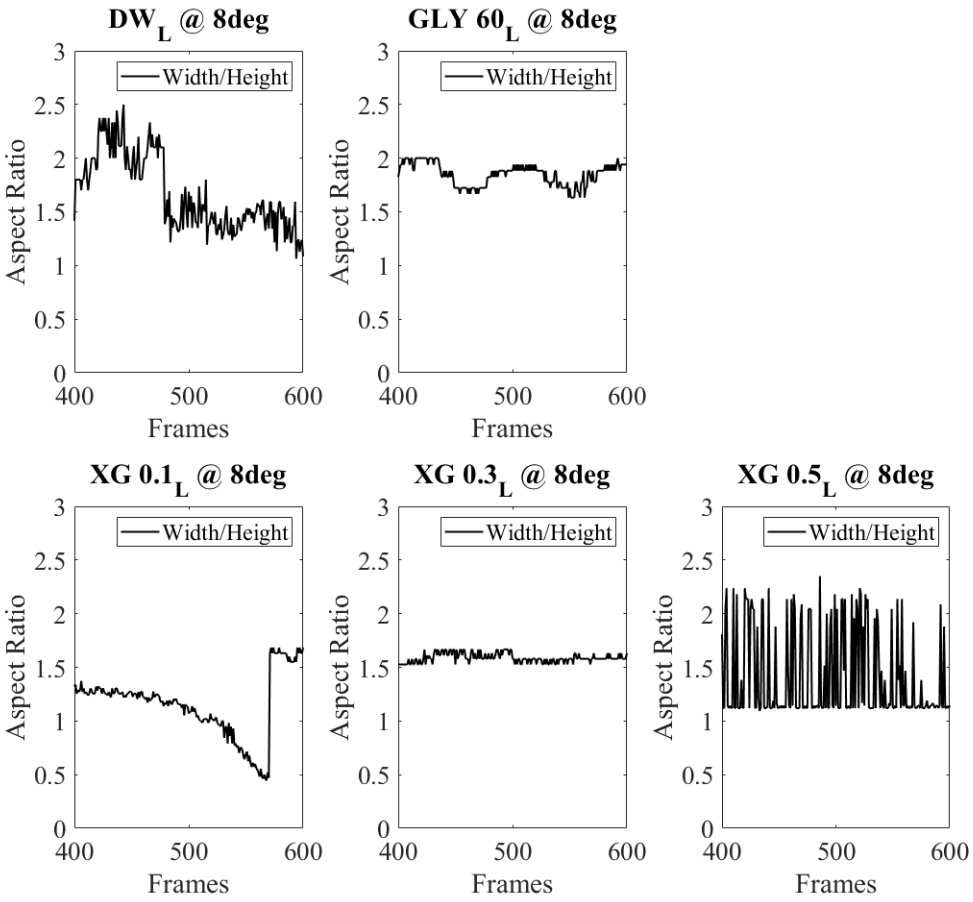

Fig. 4.11: Plot of the height divided by the width of the droplet (42.5 μL) in pixels from release on an 8° Leiden-frost plate. DW_L is distilled water, GLY 60_L is a 60% glycerin mixture, XG 0.1_L is a 0.1% xanthan mixture, XG 0.3_L is a 0.3% xanthan mixture, and XG 0.5_L is a 0.5% xanthan mixture. Each data point is taken at a point 5 inches up the plate surface.

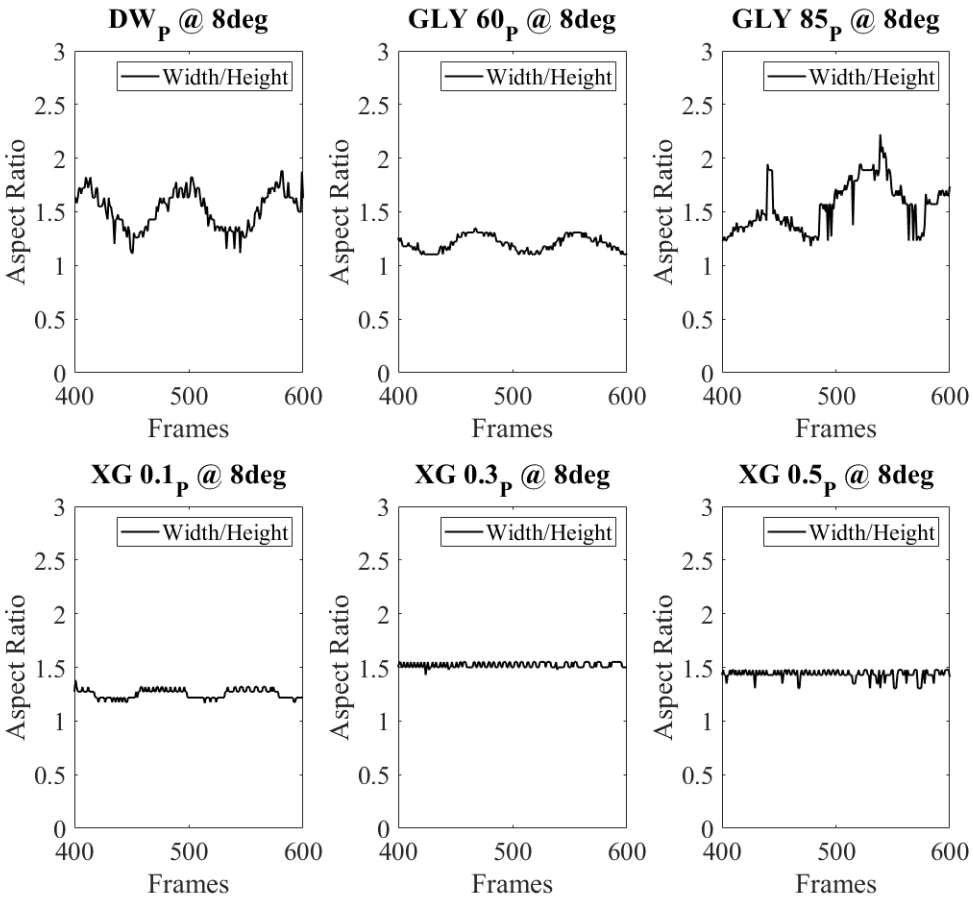

Fig. 4.12: Plot of the height divided by the width of the droplet (42.5 μL) in pixels from release on an 8° superhydrophobic plate. DW$_P$ is distilled water, GLY 60$_P$ is a 60% glycerin mixture, GLY 85$_P$ is a 85% glycerin mixture, XG 0.1$_P$ is a 0.1% xanthan mixture, XG 0.3$_P$ is a 0.3% xanthan mixture, and XG 0.5$_P$ is a 0.5% xanthan mixture. Each data point is taken at a point 5 inches up the plate surface.

CHAPTER 5

CONTRIBUTIONS AND FUTURE WORK

The hypothesis of this work is that the terminal velocity and acceleration of a droplet on an inclined plated (small angle, $< 8^{\circ}$) heated to the liedenfrost point is less dependent on viscosity than a similar droplet on a superhydrophic surface. In other words, a less viscous fluid should be faster on a hydrophobic surface and viscosity shouldn't affect velocity as much on a leidenfrost surface.

A superhydrophobic plate and a heated plate (300°C) were made of copper and droplets of water, glycerine mixtures and xanthan gum mixtures were tested on inclines betwee 2° and 8° (3.1). The results confirmed that viscosity affects the droplets rolling down the superhydrophobic plate more than the leidenfrost one. The terminal velocity was not achieved in all cases, however, there was a lower velocity for fluids with more viscosity. Most interesting were cases that were capable of exceeding the potential energy maximum speed down the plate. In the leidenfrost cases these occured at 2° and 4° degrees for water and some of the xanthan gum cases. In the superhydrophobic cases this occured only for water at 6° and 8° degrees. The cause of these excess speeds is not yet known but postulated that it is related to the altered angles affecting droplet velocity under the droplets as reported by [5].

Future work might include the following. Making a longer plate so that the terminal velocity is reached. More angles should be tested between 4° and 6° for the Leiden-frost and between 6° and 8° for the superhydrophobic cases. Measuring the shape and size of the vapor layer below the Leiden-frost droplets is an important future consideration as well as potential modeling. This would enable more accurate understanding of how much slip the droplet experiences in that region (i.e., viscous coupling). Finally, if there was a way to measure the velocity inside the droplet it might also give some insight into the external influences on the droplet motion (PIV).

REFERENCES

[1] Glycerine Producers Association, "Physical Properties of Glycerine and Its Solutions," *Proceedings of the National Academy of Sciences*, 1963.

[2] Mahadevan, L. and Pomeau, Y., "Rolling droplets," *Physics of Fluids*, Vol. 11, No. 9, 1999, pp. 2449–2453.

[3] Quéré, D., "Leidenfrost Dynamics," *Annual Review of Fluid Mechanics*, Vol. 45, No. 1, 2013, pp. 197–215.

[4] Mouterde, T., Raux, P. S., Clanet, C., and Quéré, D., "Superhydrophobic frictions," *Proceedings of the National Academy of Sciences*, Vol. 116, No. 17, 2019, pp. 8220–8223.

[5] Bouillant, A., Mouterde, T., Bourrianne, P., Lagarde, A., Clanet, C., and Quéré, D., "Leidenfrost wheels," *Nature Physics*, Vol. 14, No. 12, 2018, pp. 1188–1192.

[6] Segur, J. and Obestar, H. E., "Viscosity of Glycerol and its Aqueous Solutions," *Industrial and Engineering Chemistry*, Vol. 43, No. 9, 1951, pp. 2117–2120.

[7] Epps, B. P., Truscott, T. T., and Techet, A. H., "Evaluating derivatives of experimental data using smoothing splines," *Proceedings of Mathematical Methods in Engineering International Symposium. MMEI, Lisbon Portugal*, 2010, pp. 29–38.

APPENDICES

APPENDIX A

UNUSED BUT USEFUL FIGURES

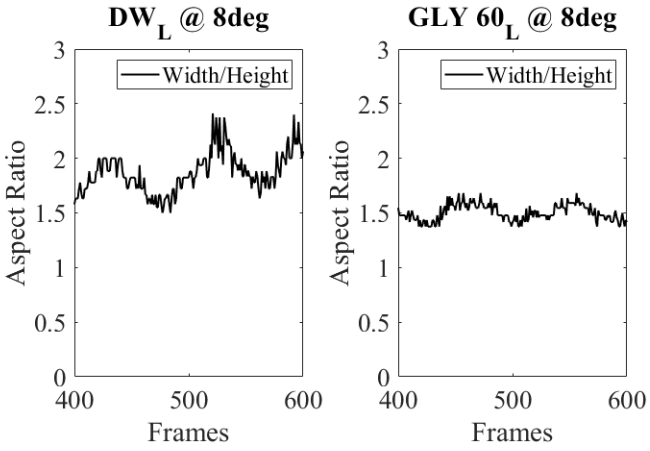

Fig. A.1: Plot of the height divided by the width in pixels from release of a 42.5μL droplet at 2 degrees.

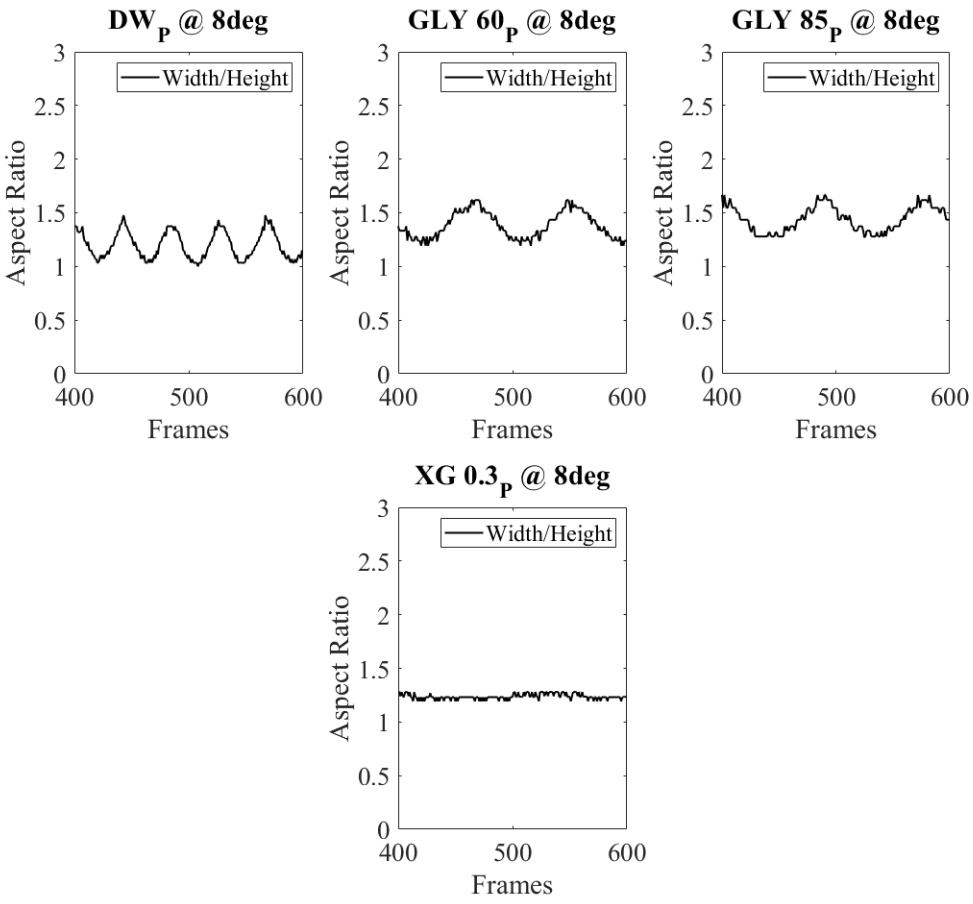

Fig. A.2: Plot of the height divided by the width in pixels from release of a a42.5μL droplet at 2 degrees.

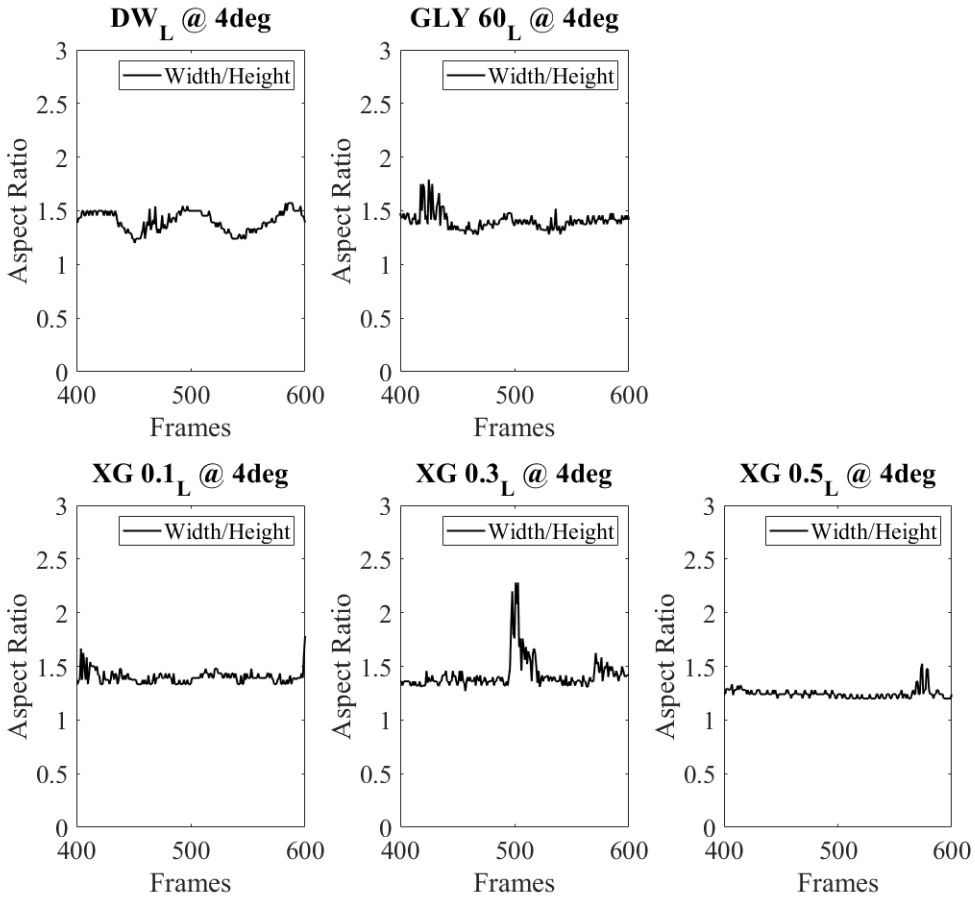

Fig. A.3: Plot of the height divided by the width in pixels from release of a 42.5μL droplet at 4 degrees.

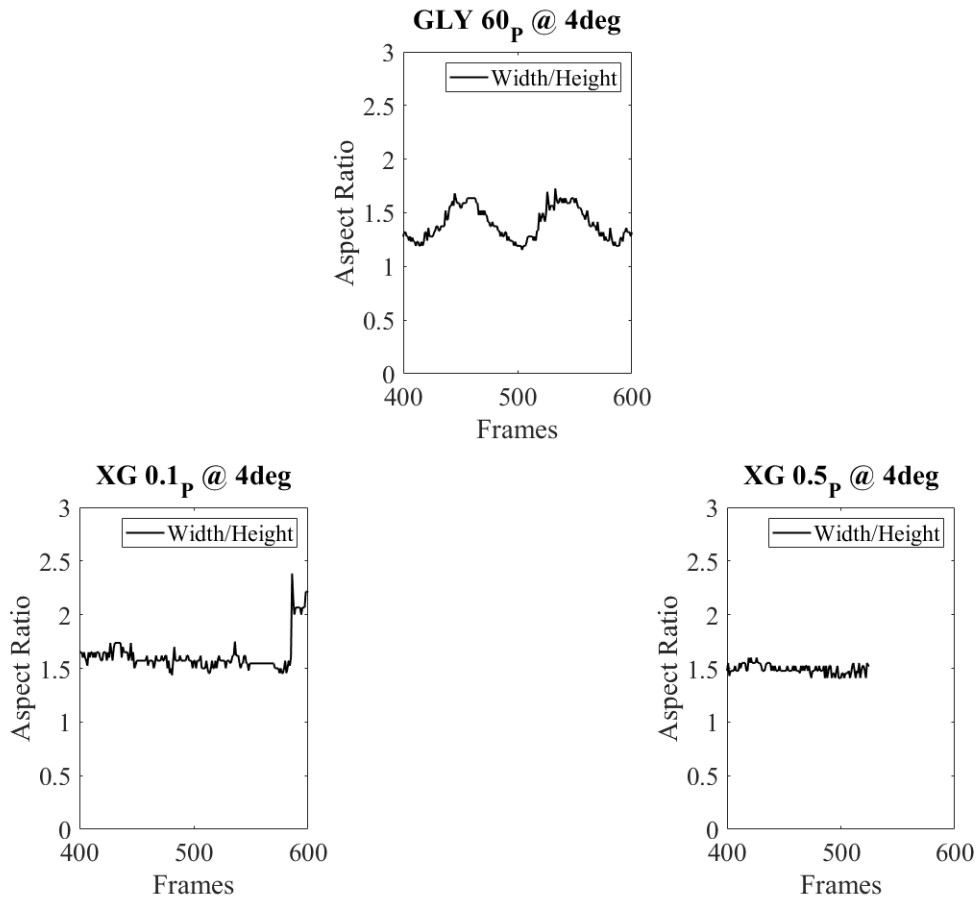

Fig. A.4: Plot of the height divided by the width in pixels from release of a 42.5μL droplet at 4 degrees.

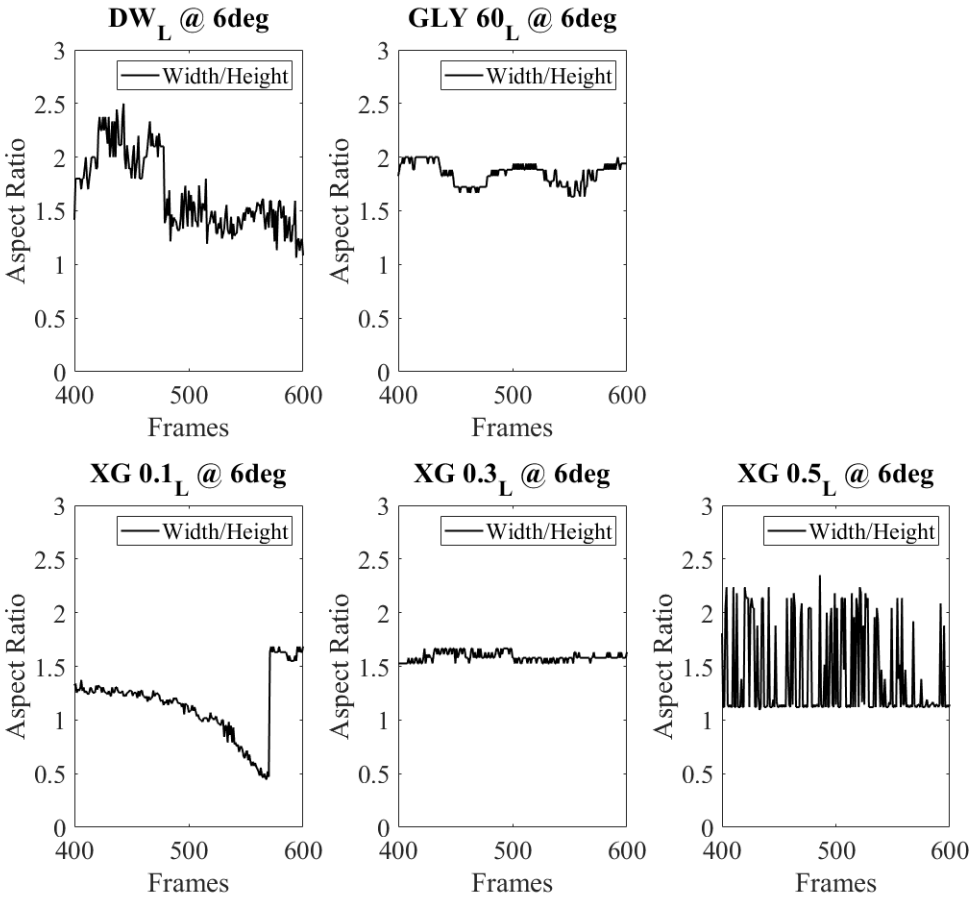

Fig. A.5: Plot of the height divided by the width in pixels from release of a 42.5μL droplet at 6 degrees.

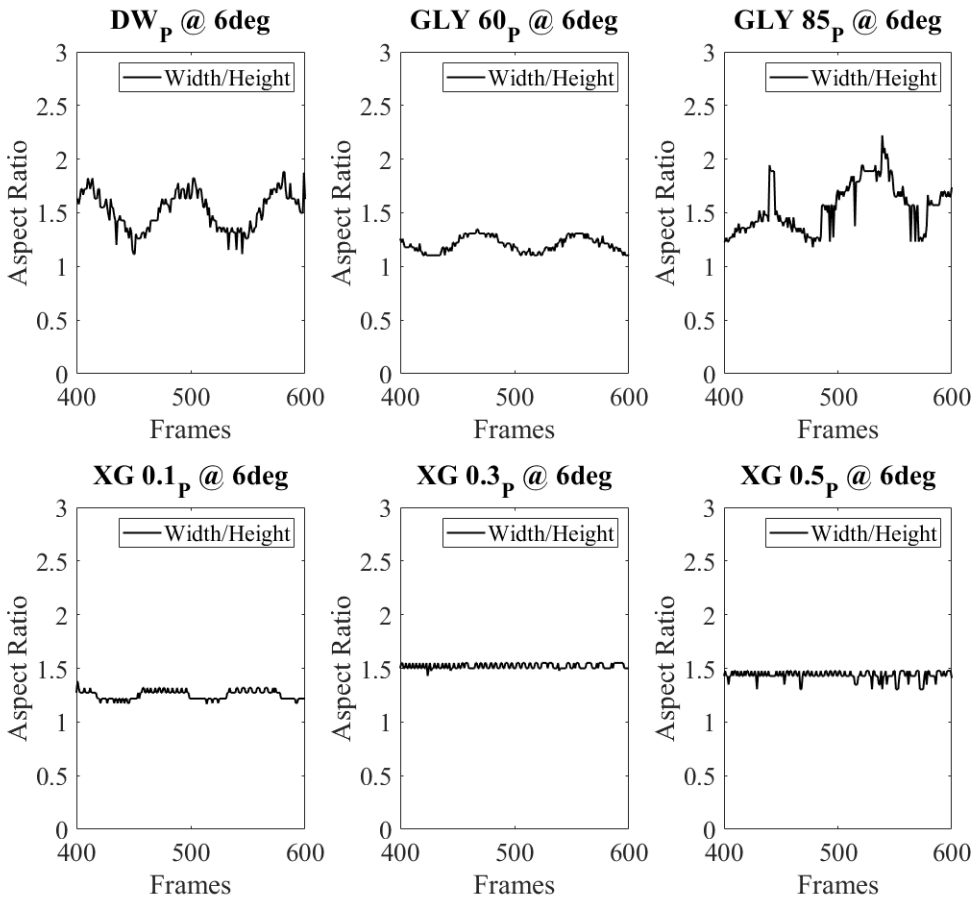

Fig. A.6: Plot of the height divided by the width in pixels from release of a 42.5μL droplet at 6 degrees.

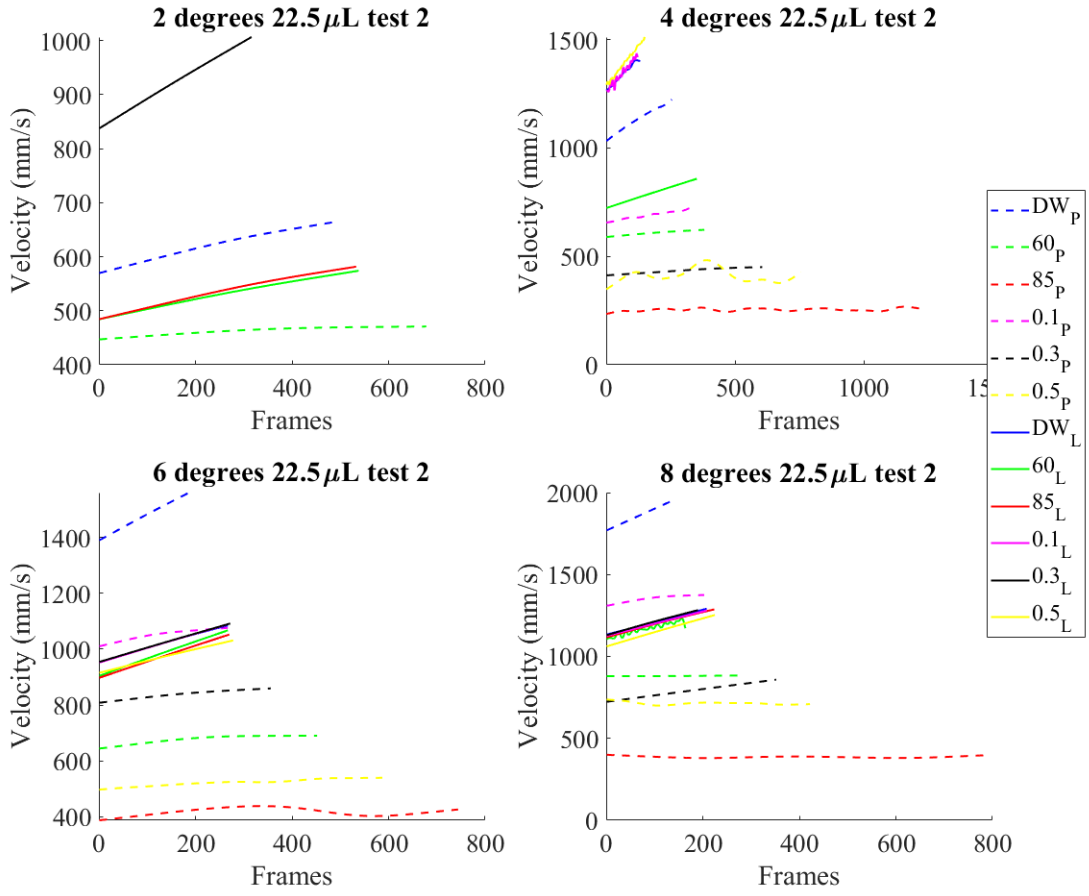

Fig. A.7: Plot of velocities for 22.5 μL of all successful droplet types.

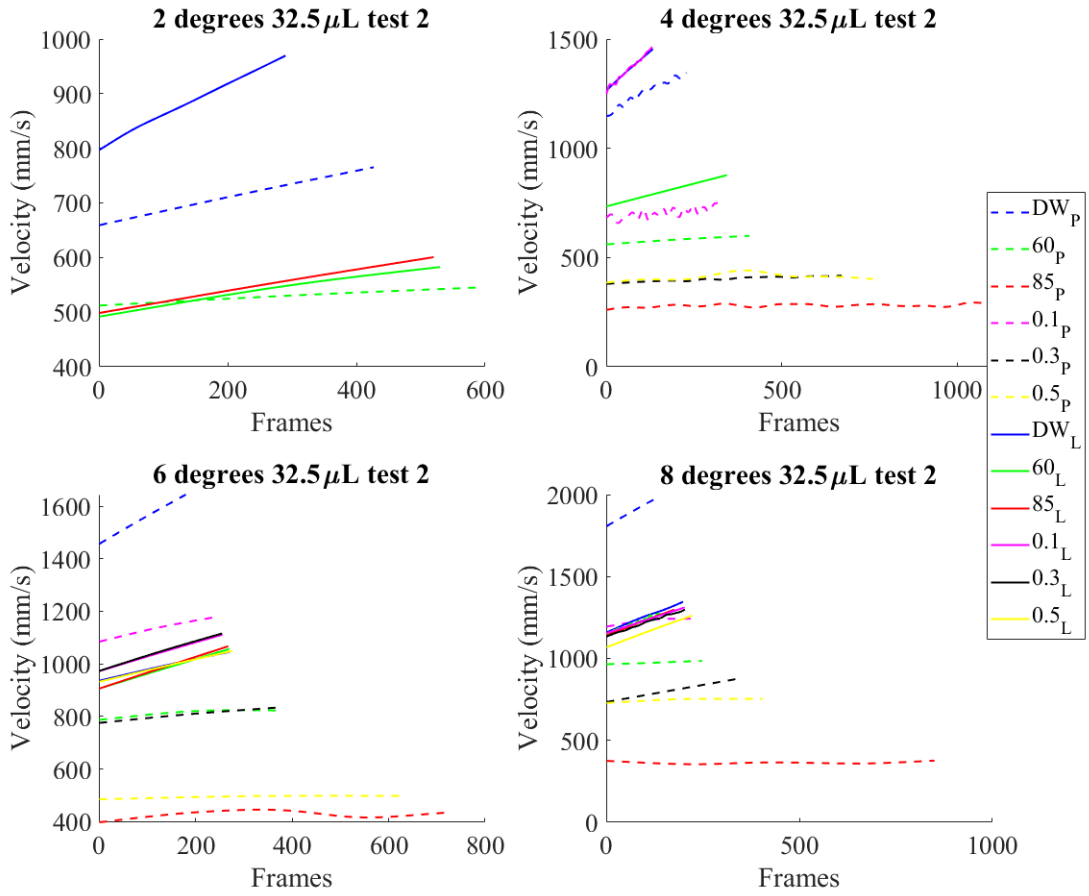

Fig. A.8: Plot of velocities for 32.5 μL of all successful droplet types.

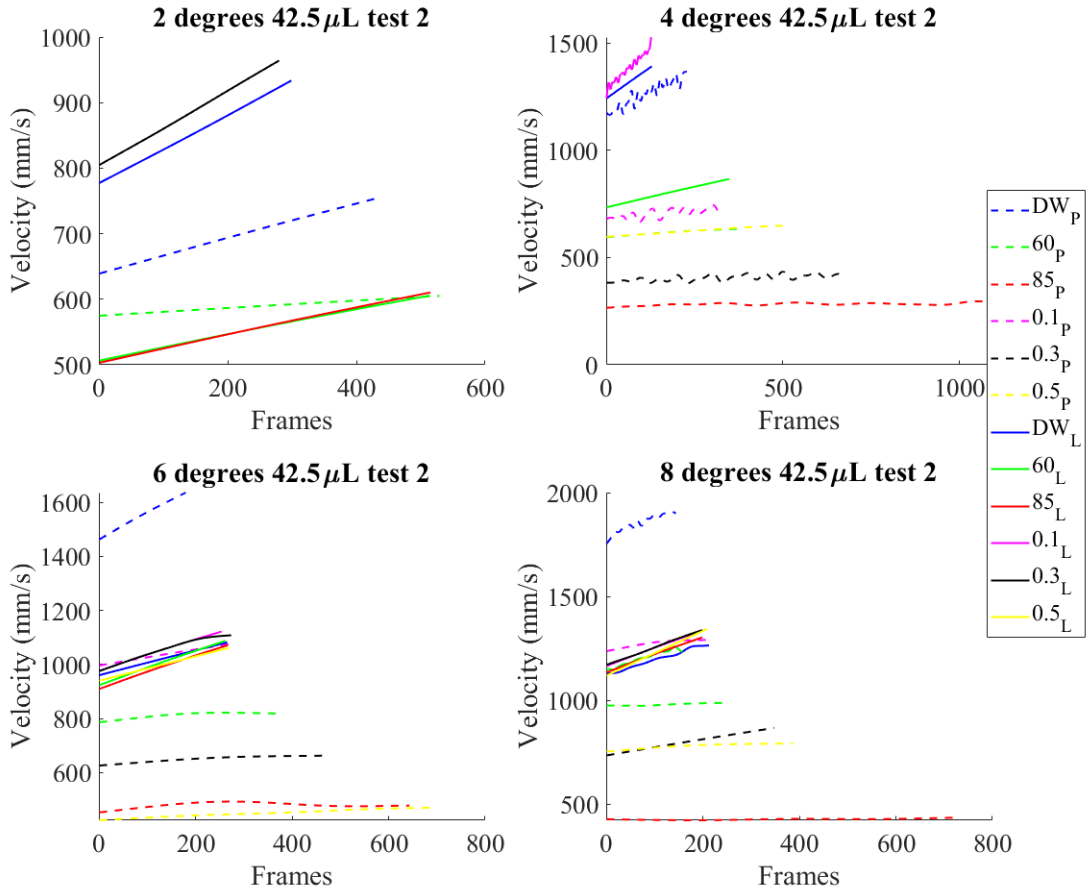

Fig. A.9: Plot of velocities for 42.5 μL of all successful droplet types.

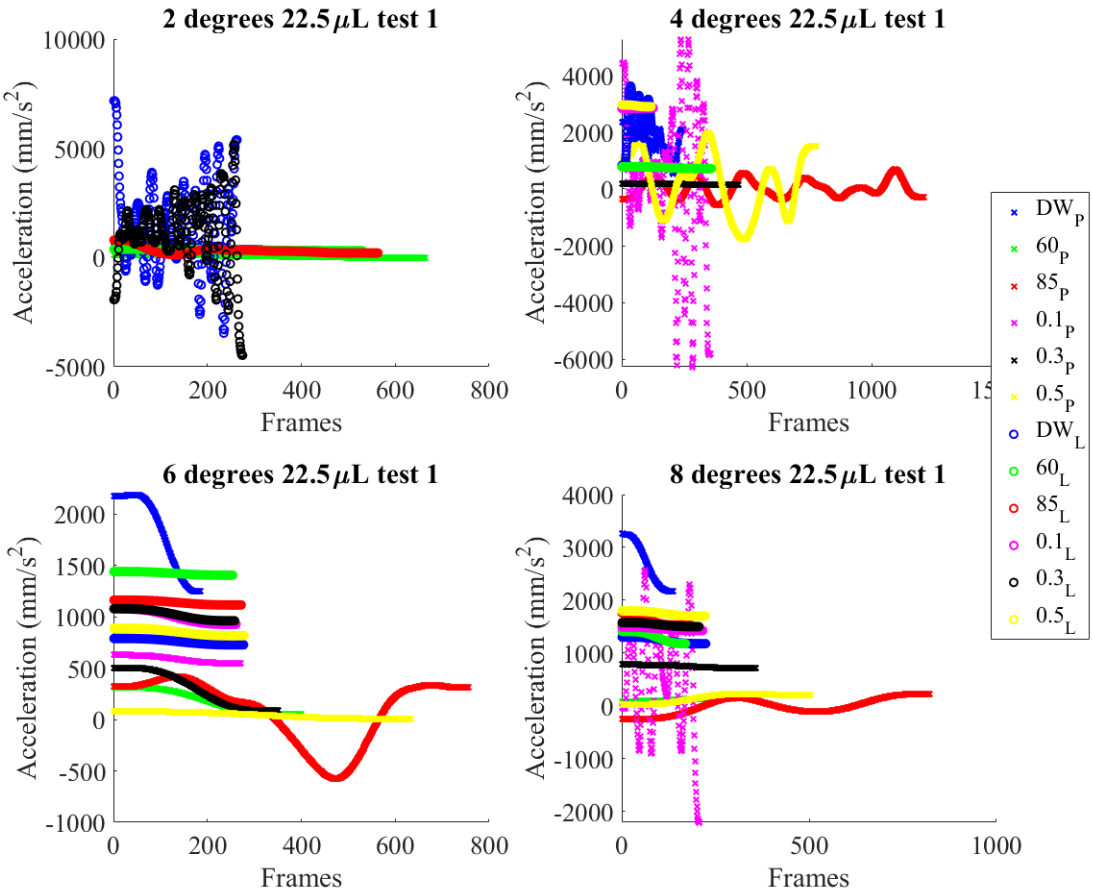

Fig. A.10: Plot of accelerations for 22.5 μL of all successful droplet types.

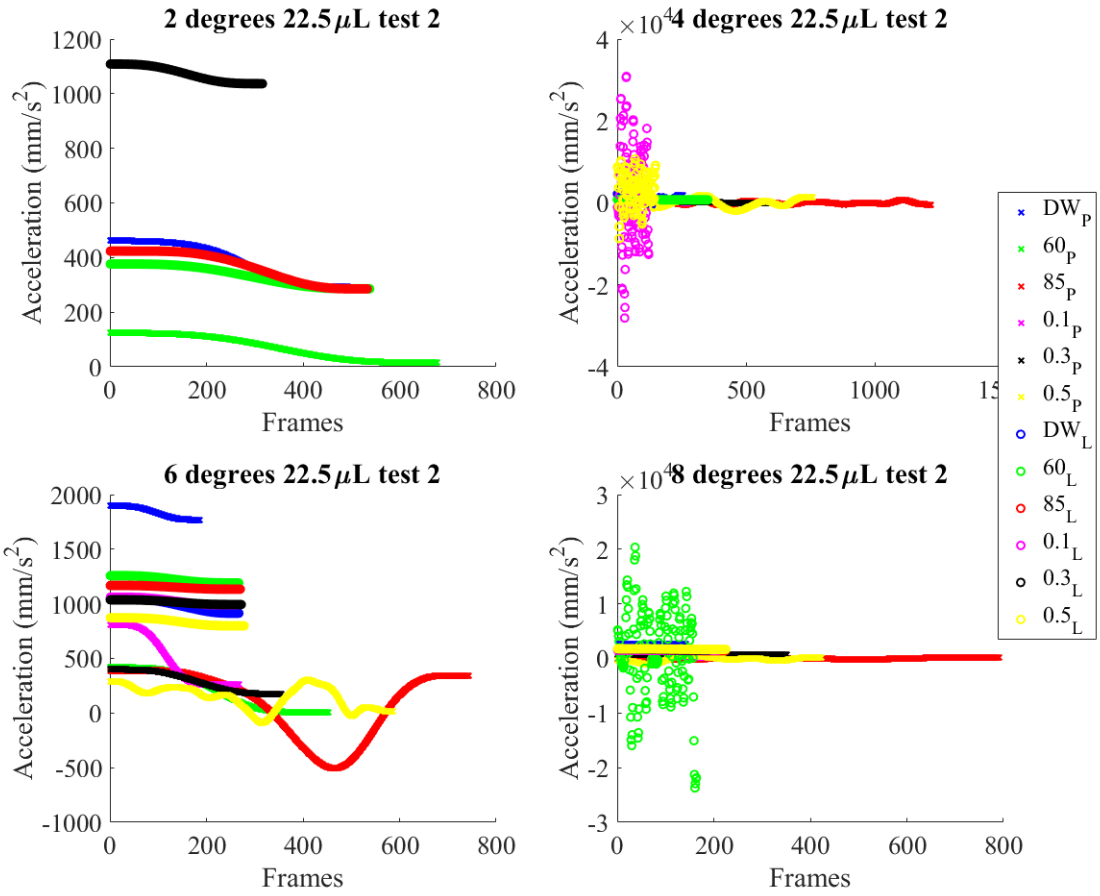

Fig. A.11: Plot of accelerations for 22.5 μL of all successful droplet types.

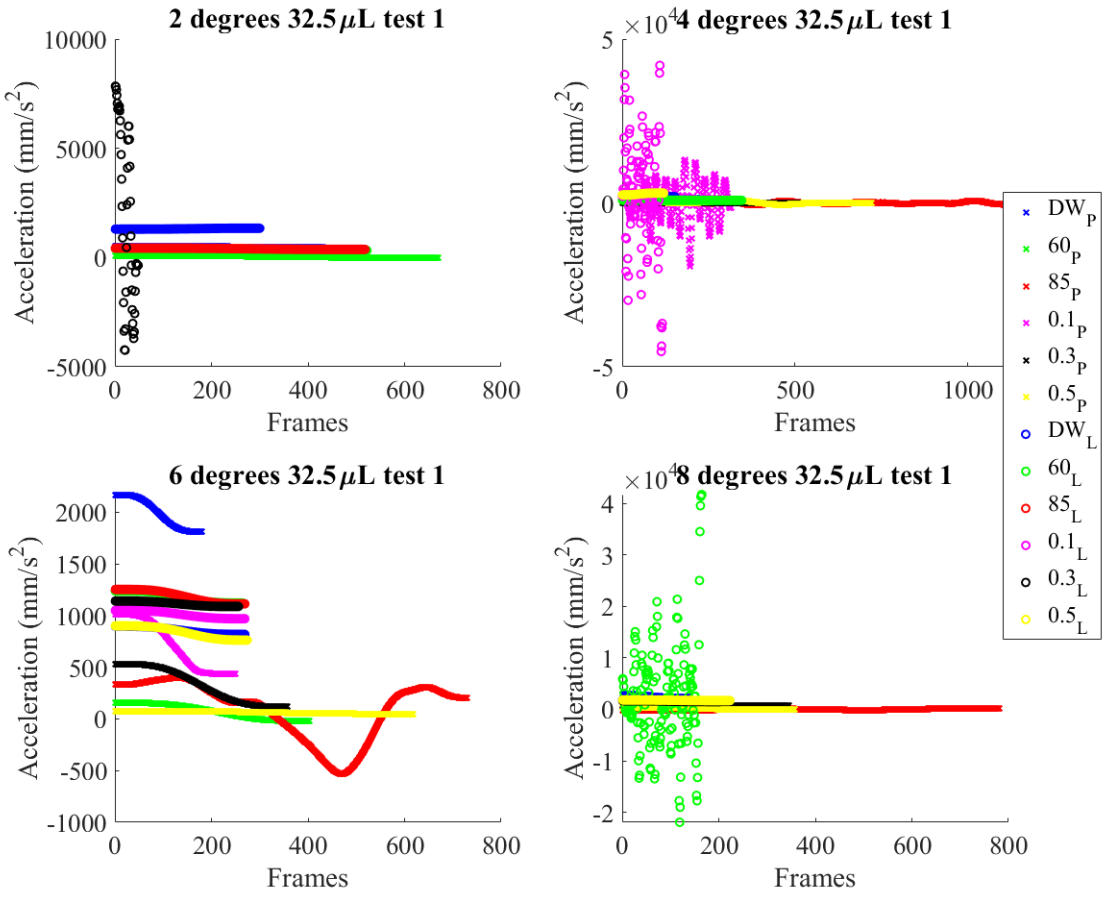

Fig. A.12: Plot of accelerations for 32.5 μL of all successful droplet types.

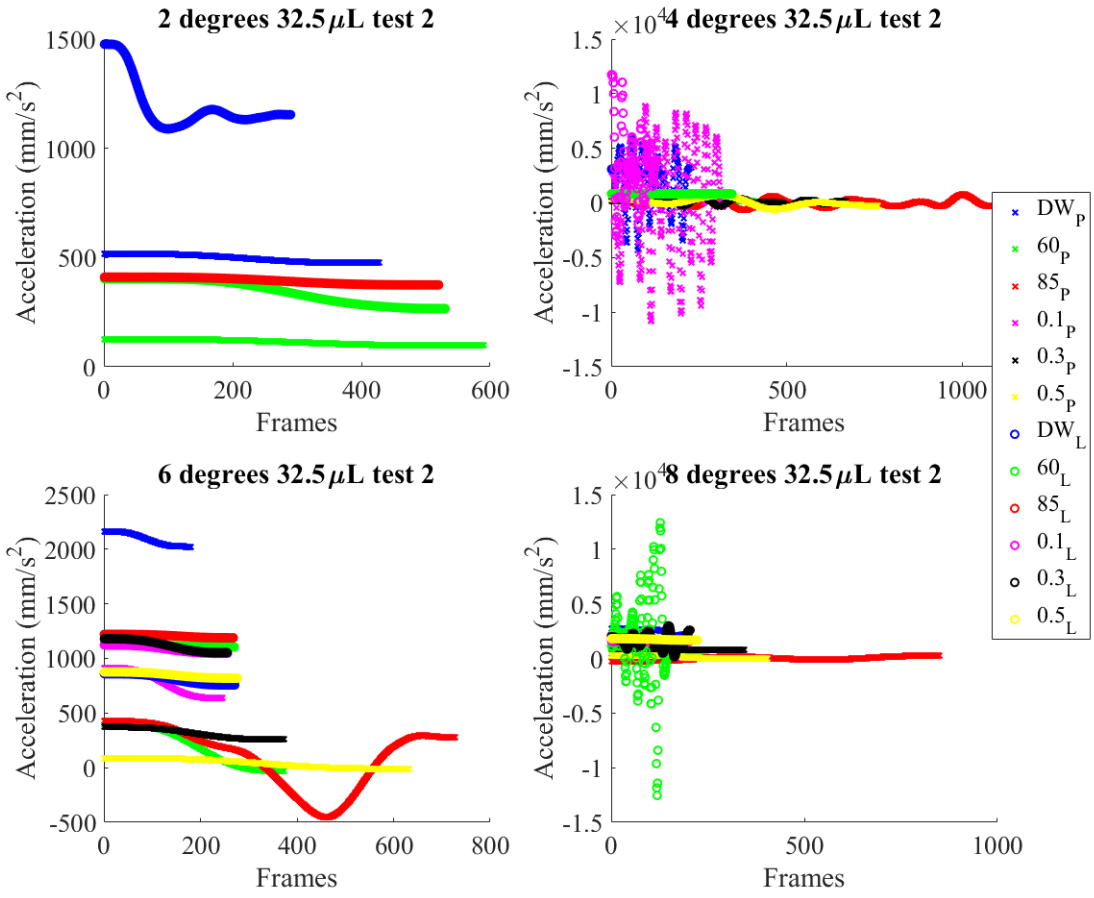

Fig. A.13: Plot of accelerations for 32.5 μL of all successful droplet types.

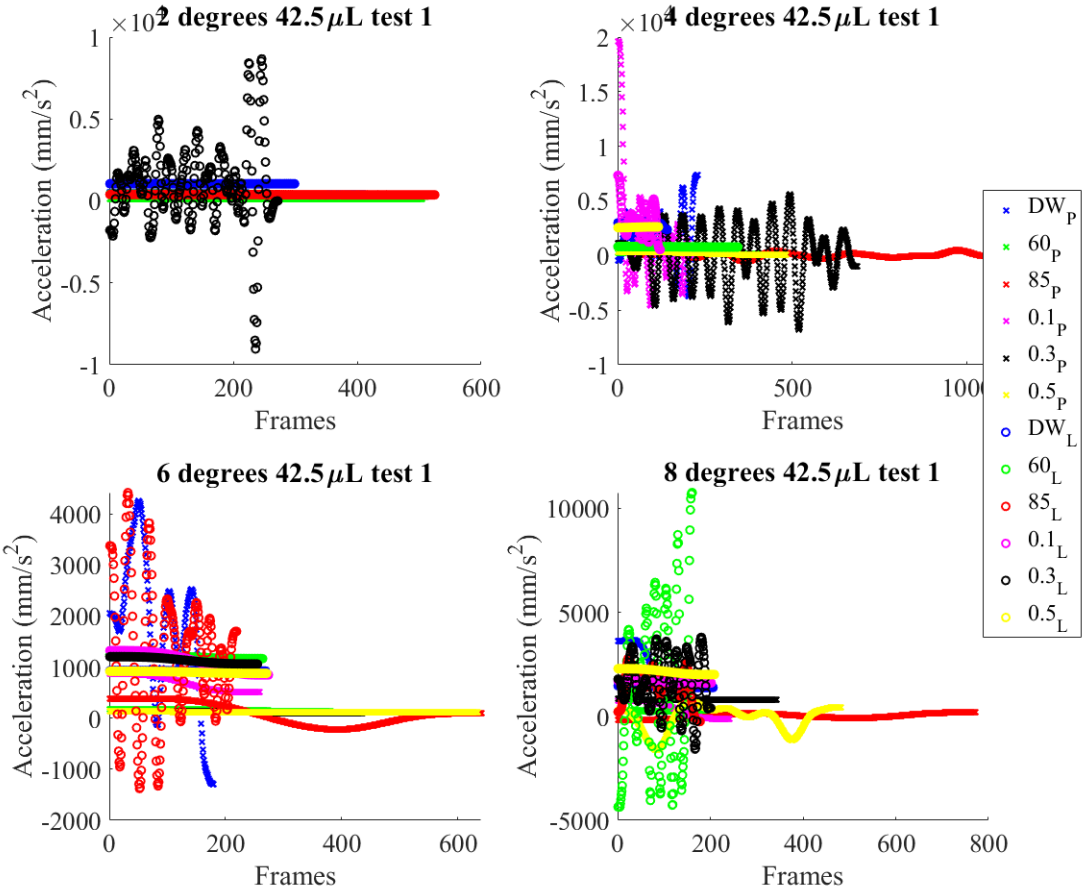

Fig. A.14: Plot of accelerations for 42.5 μL of all successful droplet types.

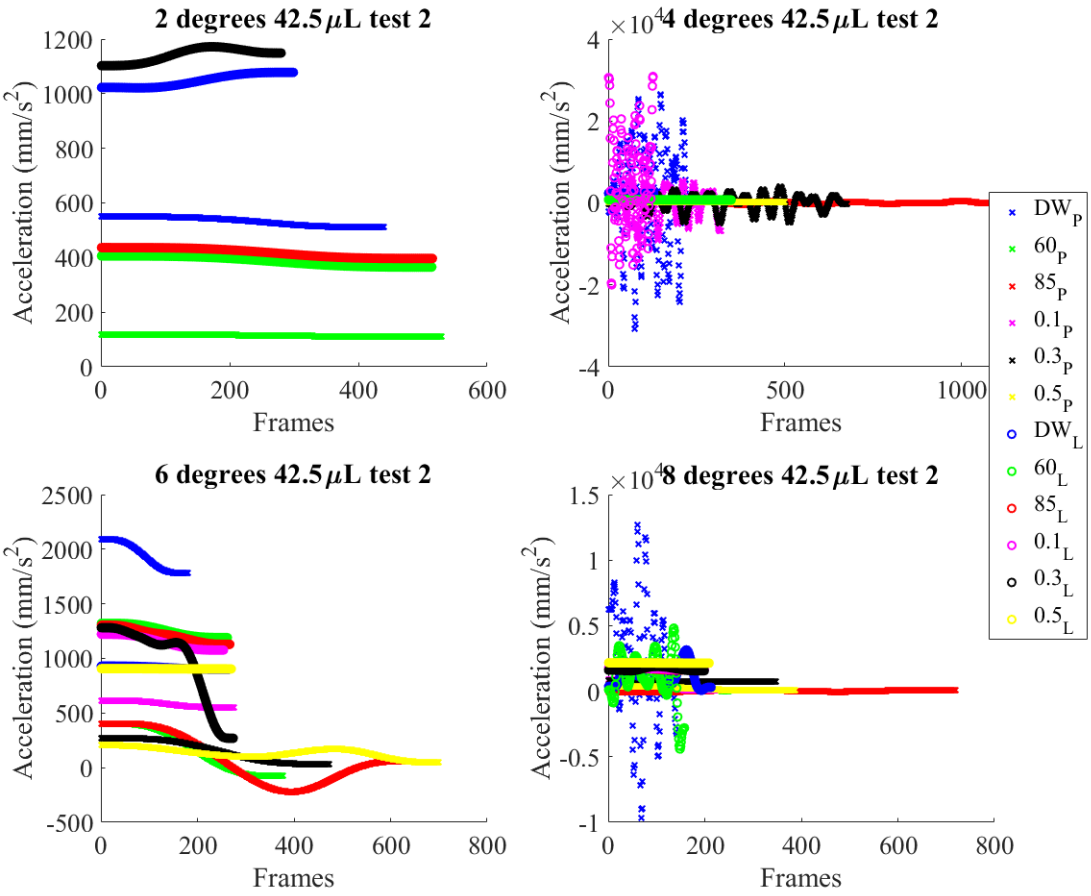

Fig. A.15: Plot of accelerations for 42.5 μL of all successful droplet types.

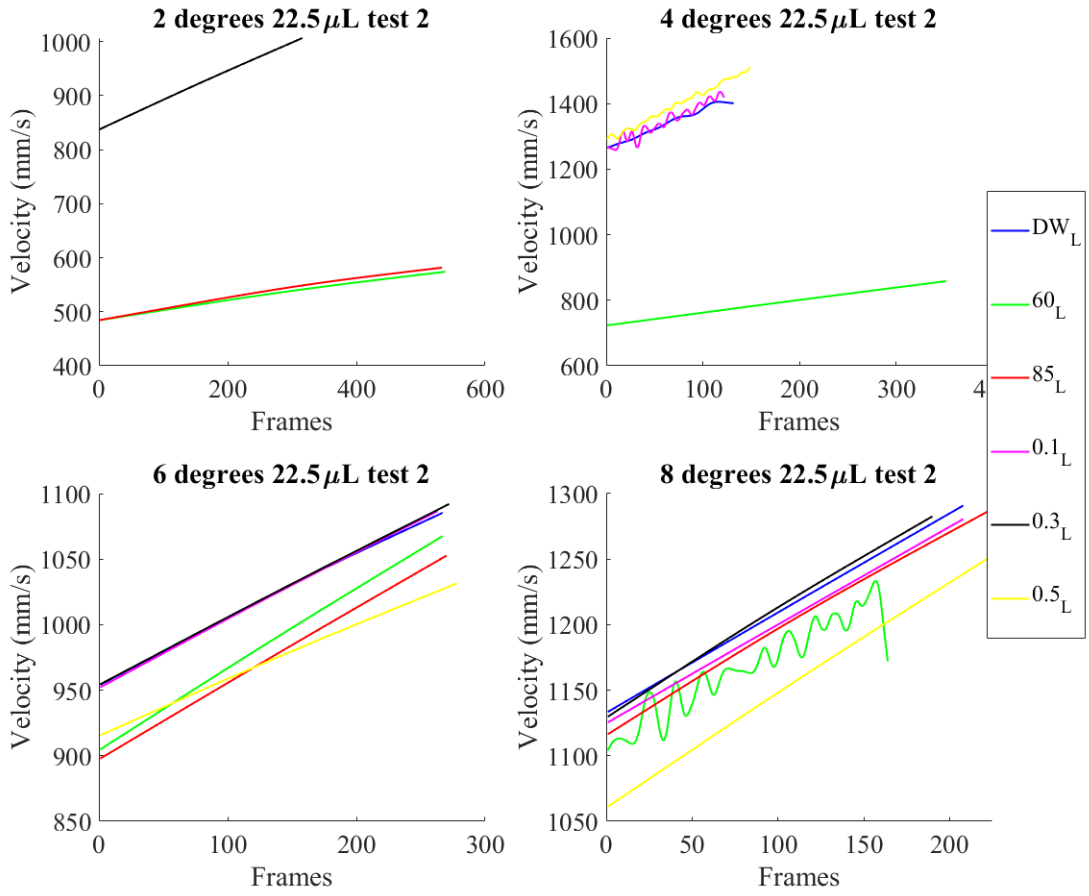

Fig. A.16: Plot of velocities on the Leidenfrost surface for 22.5 μL of all successful droplet types.

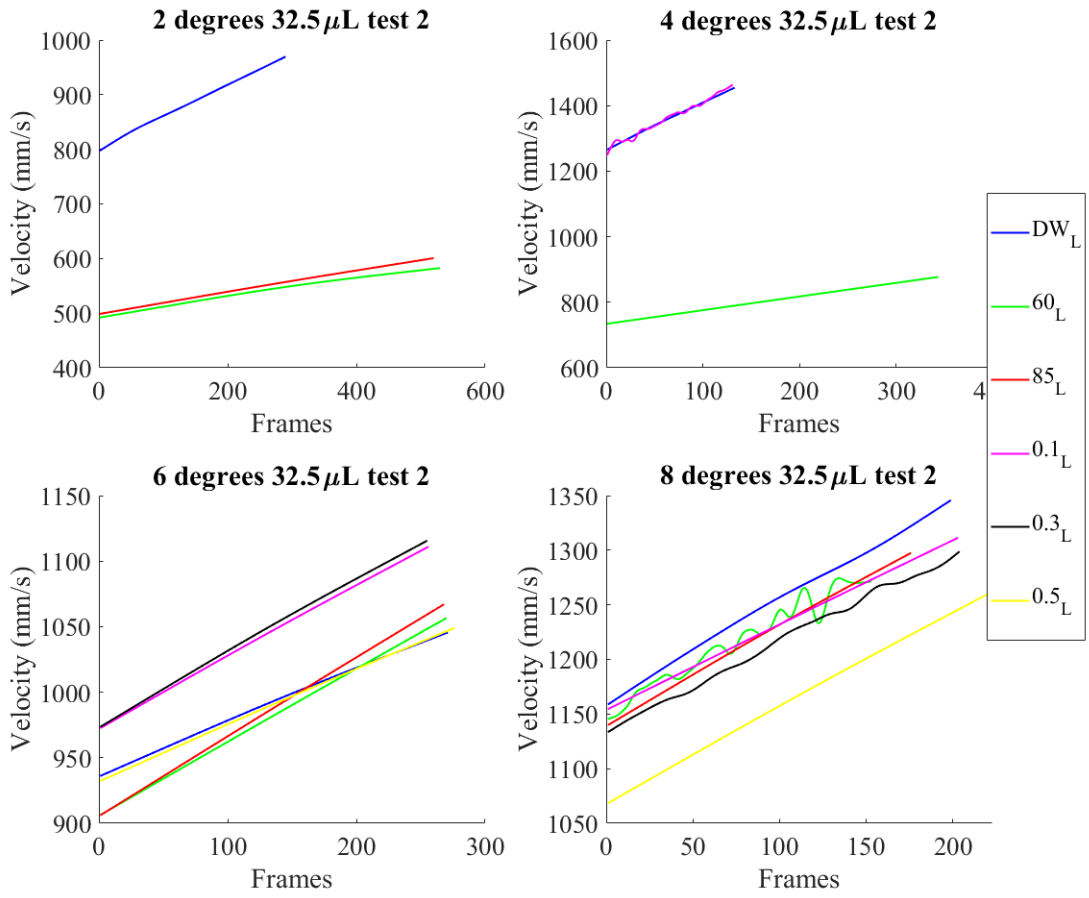

Fig. A.17: Plot of velocities on the Leidenfrost surface for 32.5 μL of all successful droplet types.

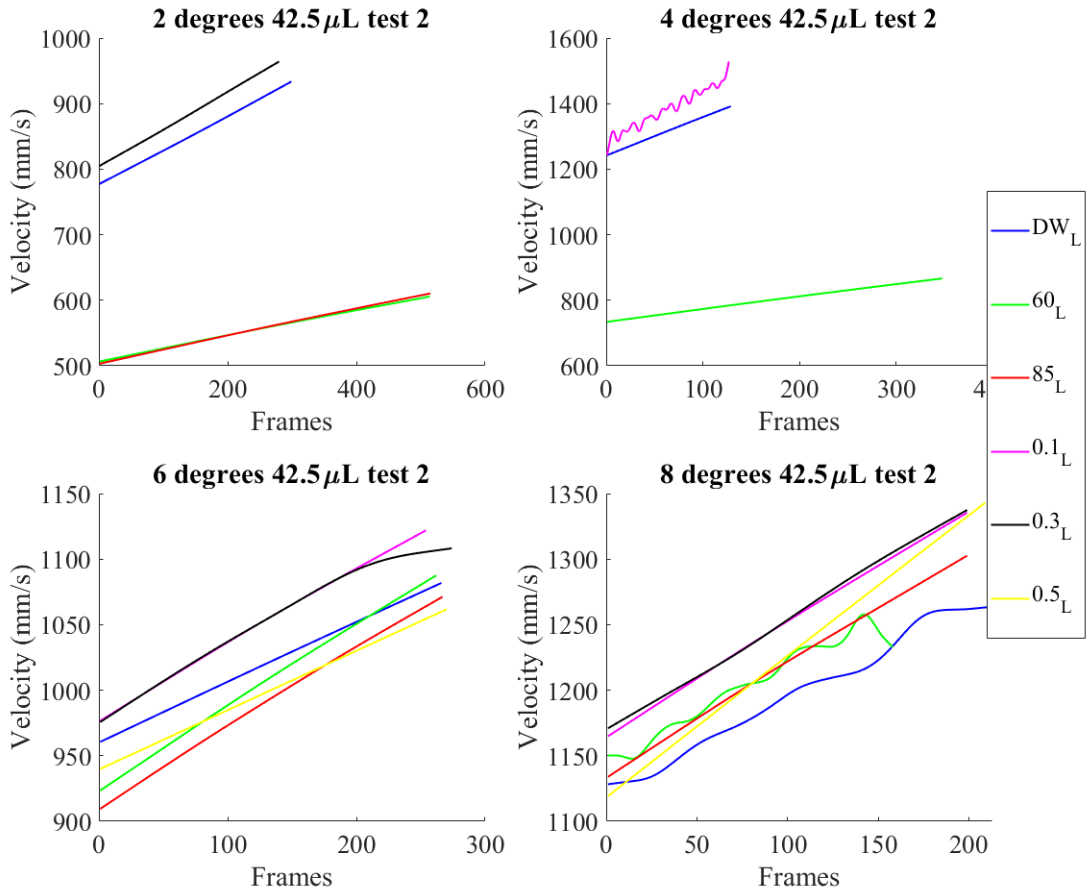

Fig. A.18: Plot of velocities on the Leidenfrost surface for 42.5 μL of all successful droplet types.